

Gaussian Belief Propagation for Solving Systems of Linear Equations: Theory and Application

Ori Shental, Danny Bickson*, Paul H. Siegel, Jack K. Wolf and Danny Dolev

Abstract

The canonical problem of solving a system of linear equations arises in numerous contexts in information theory, communication theory, and related fields. In this contribution, we develop a solution based upon Gaussian belief propagation (GaBP) that does not involve direct matrix inversion. The iterative nature of our approach allows for a distributed message-passing implementation of the solution algorithm. We address the properties of the GaBP solver, including convergence, exactness, computational complexity, message-passing efficiency and its relation to classical solution methods. We use numerical examples and applications, like linear detection, to illustrate these properties through the use of computer simulations. This empirical study demonstrates the attractiveness (*e.g.*, faster convergence rate) of the proposed GaBP solver in comparison to conventional linear-algebraic iterative solution methods.

Index Terms

Belief propagation, sum-product, system of linear equations, probabilistic inference, max-product, Gaussian elimination, iterative solution methods, Moore-Penrose pseudoinverse, linear detection, Poisson's equation.

The first two authors contributed equally to this work.

O. Shental, P. H. Siegel and J. K. Wolf are with the Center for Magnetic Recording Research (CMRR), University of California - San Diego (UCSD), 9500 Gilman Drive, La Jolla, CA 92093, USA (Email: {oshental,psiegel,jwolf}@ucsd.edu).

* Contact Author. D. Bickson and D. Dolev are with the School of Computer Science and Engineering, Hebrew University of Jerusalem, Jerusalem 91904, Israel (Email: {daniel51,dolev}@cs.huji.ac.il).

The material in this paper was presented in part at the forty-fifth Annual Allerton Conference on Communication, Control, and Computing, September 2007 and on the IEEE International Symposium on Information Theory (ISIT), July 2008.

Paper submitted to IEEE Transactions on Information Theory, November 1, 2018.

I. INTRODUCTION

Solving a system of linear equations $\mathbf{Ax} = \mathbf{b}$ is one of the most fundamental problems in algebra, with countless applications in the mathematical sciences and engineering. Given an observation vector $\mathbf{b} \in \mathbb{R}^m$ and the data matrix $\mathbf{A} \in \mathbb{R}^{m \times n}$ ($m \geq n \in \mathbb{Z}$), a unique solution, $\mathbf{x} = \mathbf{x}^* \in \mathbb{R}^n$, exists if and only if the data matrix \mathbf{A} has full column rank. Assuming a nonsingular matrix \mathbf{A} , the system of equations can be solved either directly or in an iterative manner. Direct matrix inversion methods, such as Gaussian elimination (LU factorization, [1]-Ch. 3) or band Cholesky factorization ([1]-Ch. 4), find the solution with a finite number of operations, typically, for a dense $n \times n$ matrix, of the order of n^3 . The former is particularly effective for systems with unstructured dense data matrices, while the latter is typically used for structured dense systems.

Iterative methods [2] are inherently simpler, requiring only additions and multiplications, and have the further advantage that they can exploit the sparsity of the matrix \mathbf{A} to reduce the computational complexity as well as the algorithmic storage requirements [3]. By comparison, for large, sparse and amorphous data matrices, the direct methods are impractical due to the need for excessive matrix reordering operations.

The main drawback of the iterative approaches is that, under certain conditions, they converge only asymptotically to the exact solution \mathbf{x}^* [2]. Thus, there is the risk that they may converge slowly, or not at all. In practice, however, it has been found that they often converge to the exact solution or a good approximation after a relatively small number of iterations.

A powerful and efficient iterative algorithm, belief propagation (BP, [4]), also known as the sum-product algorithm, has been very successfully used to solve, either exactly or approximately, inference problems in probabilistic graphical models [5].

In this paper, we reformulate the general problem of solving a linear system of algebraic equations as a probabilistic inference problem on a suitably-defined graph. We believe that this is the first time that an explicit connection between these two ubiquitous problems has been established¹. Furthermore, for the first time, we provide a full step-by-step derivation of the GaBP algorithm from the belief propagation algorithm.

¹Recently, we have found out the work of Moallemi and Van Roy [6] which discusses the connection between the Min-Sum message passing algorithm and solving quadratic programs. Both works [6], [7] were published in parallel, and the algorithms were derived independently, using different techniques. In Appendix IV we discuss the connection between the two algorithms, and show they are equivalent.

As an important consequence, we demonstrate that Gaussian BP (GaBP) provides an efficient, distributed approach to solving a linear system that circumvents the potentially complex operation of direct matrix inversion. Using the seminal work of Weiss and Freeman [8] and some recent related developments [6], [7], [9]–[12], we address the convergence and exactness properties of the proposed GaBP solver. Other properties of the GaBP solver, as computational complexity, message-passing efficiency and its relation to classical solution methods are also investigated.

As application of this new approach to solving a system of linear equations, we consider the problem of linear detection using a decorrelator in a code-division multiple-access (CDMA) system. Through the use of the iterative message-passing formulation, we implement the decorrelator detector in a distributed manner. This example allows us to quantitatively compare the new GaBP solver with the classical iterative solution methods that have been previously investigated in the context of a linear implementation of CDMA demodulation [13]–[15]. We show that the GaBP-based decorrelator yields faster convergence than these conventional methods. Furthermore, the GaBP convergence is further accelerated by incorporating the linear-algebraic methods of Aitken and Steffensen [16] into the GaBP-based scheme. As far as we know, this represents the first time these acceleration methods have been examined within the framework of message-passing algorithms.

The paper is organized as follows. We introduce the problem model in Section II. In Section III, we derive the distributed GaBP-based solution method and address its convergence and exactness properties in Section IV. We discuss the algorithm complexity and message passing efficiency in Section V. The relation to classical linear algebra solution methods is explored in Section VI. In Section VIII, we outline numerical examples and use the linear detection problem to illustrate experimentally the superior convergence rate of the GaBP solver, relative to conventional iterative methods. Concluding remarks are presented in Section X.

II. PRELIMINARIES: NOTATIONS AND DEFINITIONS

A. Linear Algebra

We shall use the following linear-algebraic notations and definitions. The operator $\{\cdot\}^T$ stands for a vector or matrix transpose, the matrix \mathbf{I}_n is an $n \times n$ identity matrix, while the symbols $\{\cdot\}_i$ and $\{\cdot\}_{ij}$ denote entries of a vector and matrix, respectively. Let $\mathbf{M} \in \mathbb{R}^{n \times n}$ be a real symmetric square matrix and $\mathbf{A} \in \mathbb{R}^{m \times n}$ be a real (possibly rectangular) matrix. Let

Definition 1 (Pseudoinverse): The Moore-Penrose pseudoinverse matrix of the matrix \mathbf{A} , denoted by \mathbf{A}^\dagger , is defined as

$$\mathbf{A}^\dagger \triangleq (\mathbf{A}^T \mathbf{A})^{-1} \mathbf{A}^T. \quad (1)$$

Definition 2 (Spectral radius): The spectral radius of the matrix \mathbf{M} , denoted by $\rho(\mathbf{M})$, is defined to be the maximum of the absolute values of the eigenvalues of \mathbf{M} , i.e.,

$$\rho(\mathbf{M}) \triangleq \max_{1 \leq i \leq s} (|\lambda_i|), \quad (2)$$

where $\lambda_1, \dots, \lambda_s$ are the eigenvalues of the matrix \mathbf{M} .

Definition 3 (Diagonal dominance): The matrix \mathbf{M} is

1) weakly diagonally dominant if

$$|M_{ii}| \geq \sum_{j \neq i} |M_{ij}|, \forall i, \quad (3)$$

2) strictly diagonally dominant if

$$|M_{ii}| > \sum_{j \neq i} |M_{ij}|, \forall i, \quad (4)$$

3) irreducibly diagonally dominant if \mathbf{M} is irreducible², and

$$|M_{ii}| \geq \sum_{j \neq i} |M_{ij}|, \forall i, \quad (5)$$

with strict inequality for at least one i .

Definition 4 (PSD): The matrix \mathbf{M} is positive semi-definite (PSD) if and only if for all non-zero real vectors $\mathbf{z} \in \mathbb{R}^n$,

$$\mathbf{z}^T \mathbf{M} \mathbf{z} \geq 0. \quad (6)$$

Definition 5 (Residual): For a real vector $\mathbf{x} \in \mathbb{R}^n$, the residual, $\mathbf{r} = \mathbf{r}(\mathbf{x}) \in \mathbb{R}^m$, of a linear system is $\mathbf{r} = \mathbf{A}\mathbf{x} - \mathbf{b}$.

The standard norm of the residual, $\|\mathbf{r}\|_p (p = 1, 2, \dots, \infty)$, is a good measure of the accuracy of a vector \mathbf{x} as a solution to the linear system. In our experimental study, the Frobenius norm (i.e., $p = 2$) per equation is used, $\|\mathbf{r}\|_F/m = \sqrt{\sum_{i=1}^m r_i^2}/m$.

Definition 6: The condition number, κ , of the matrix \mathbf{M} is defined as

$$\kappa_p \triangleq \|\mathbf{M}\|_p \|\mathbf{M}\|_p^{-1}. \quad (7)$$

² A matrix is said to be reducible if there is a permutation matrix \mathbf{P} such that \mathbf{PMP}^T is block upper triangular. Otherwise, it is irreducible.

For \mathbf{M} being a normal matrix (i.e., $\mathbf{M}^T\mathbf{M} = \mathbf{M}\mathbf{M}^T$), the condition number is given by

$$\kappa = \kappa_2 = \left| \frac{\lambda_{\max}}{\lambda_{\min}} \right|, \quad (8)$$

where λ_{\max} and λ_{\min} are the maximal and minimal eigenvalues of \mathbf{M} , respectively.

Even though a system is nonsingular it could be ill-conditioned. Ill-conditioning means that a small perturbation in the data matrix \mathbf{A} , or the observation vector \mathbf{b} , causes large perturbations in the solution, \mathbf{x}^* . This determines the difficulty of solving the problem. The condition number is a good measure of the ill-conditioning of the matrix. The better the conditioning of a matrix the condition number is smaller, going to unity. The condition number of a non-invertible (singular) matrix is set arbitrarily to infinity.

B. Graphical Models

We will make use of the following terminology and notation in the discussion of the GaBP algorithm. Given the data matrix \mathbf{A} and the observation vector \mathbf{b} , one can write explicitly the Gaussian density function, $p(\mathbf{x})$, and its corresponding graph \mathcal{G} consisting of edge potentials (compatibility functions) ψ_{ij} and self potentials ('evidence') ϕ_i . These graph potentials are simply determined according to the following pairwise factorization of the Gaussian function (11)

$$p(\mathbf{x}) \propto \prod_{i=1}^n \phi_i(x_i) \prod_{\{i,j\}} \psi_{ij}(x_i, x_j), \quad (9)$$

resulting in $\psi_{ij}(x_i, x_j) \triangleq \exp(-x_i A_{ij} x_j)$ and $\phi_i(x_i) \triangleq \exp(b_i x_i - A_{ii} x_i^2 / 2)$. The edges set $\{i, j\}$ includes all non-zero entries of \mathbf{A} for which $i > j$. The set of graph nodes $\mathbf{N}(i)$ denotes the set of all the nodes neighboring the i th node (excluding node i). The set $\mathbf{N}(i) \setminus j$ excludes the node j from $\mathbf{N}(i)$.

C. Problem Formulation

Let $\mathbf{A} \in \mathbb{R}^{m \times n}$ ($m, n \in \mathbb{N}^*$) be a full column rank, $m \times n$ real-valued matrix, with $m \geq n$, and let $\mathbf{b} \in \mathbb{R}^m$ be a real-valued vector. Our objective is to efficiently find a solution \mathbf{x}^* to the linear system of equations $\mathbf{A}\mathbf{x} = \mathbf{b}$ given by

$$\mathbf{x}^* = \mathbf{A}^\dagger \mathbf{b}. \quad (10)$$

Throughout the development in this contribution, we make the following assumption.

Assumption 7: The matrix \mathbf{A} is square (i.e., $m = n$) and symmetric.

For the case of square matrices the pseudoinverse matrix is nothing but the data matrix inverse, *i.e.*, $\mathbf{A}^\dagger = \mathbf{A}^{-1}$. For any linear system of equations with a unique solution, Assumption 7 conceptually entails no loss of generality, as can be seen by considering the invertible system defined by the new symmetric (and PSD) matrix $\mathbf{A}_{n \times m}^T \mathbf{A}_{m \times n} \mapsto \mathbf{A}_{n \times n}$ and vector $\mathbf{A}_{n \times m}^T \mathbf{b}_{m \times 1} \mapsto \mathbf{b}_{n \times 1}$. However, this transformation involves an excessive computational complexity of $\mathcal{O}(n^2m)$ and $\mathcal{O}(nm)$ operations, respectively. Furthermore, a sparse data matrix may become dense due to the transformation, an undesired property as far as complexity concerns. Thus, we first limit the discussion to the solution of the popular case of square matrices. In Section VII the proposed GaBP solver is extended to the more general case of linear systems with rectangular $m \times n$ full rank matrices.

III. THE GABP-BASED SOLVER DERIVATION

A. From Linear Algebra to Probabilistic Inference

We begin our derivation by defining an undirected graphical model (*i.e.*, a Markov random field), \mathcal{G} , corresponding to the linear system of equations. Specifically, let $\mathcal{G} = (\mathcal{X}, \mathcal{E})$, where \mathcal{X} is a set of nodes that are in one-to-one correspondence with the linear system's variables $\mathbf{x} = \{x_1, \dots, x_n\}^T$, and where \mathcal{E} is a set of undirected edges determined by the non-zero entries of the (symmetric) matrix \mathbf{A} .

Using this graph, we can translate the problem of solving the linear system from the algebraic domain to the domain of probabilistic inference, as stated in the following theorem.

Proposition 8: The computation of the solution vector \mathbf{x}^* is identical to the inference of the vector of marginal means $\mu \triangleq \{\mu_1, \dots, \mu_n\}$ over the graph \mathcal{G} with the associated joint Gaussian probability density function $p(\mathbf{x}) \sim \mathcal{N}(\mu, \mathbf{A}^{-1})$.

Proof: [**Proof**] Another way of solving the set of linear equations $\mathbf{A}\mathbf{x} - \mathbf{b} = \mathbf{0}$ is to represent it by using a quadratic form $q(\mathbf{x}) \triangleq \mathbf{x}^T \mathbf{A}\mathbf{x}/2 - \mathbf{b}^T \mathbf{x}$. As the matrix \mathbf{A} is symmetric, the derivative of the quadratic form w.r.t. the vector \mathbf{x} is given by the vector $\partial q/\partial \mathbf{x} = \mathbf{A}\mathbf{x} - \mathbf{b}$. Thus equating $\partial q/\partial \mathbf{x} = \mathbf{0}$ gives the global minimum \mathbf{x}^* of this convex function, which is nothing but the desired solution to $\mathbf{A}\mathbf{x} = \mathbf{b}$.

Next, one can define the following joint Gaussian probability density function

$$p(\mathbf{x}) \triangleq \mathcal{Z}^{-1} \exp(-q(\mathbf{x})) = \mathcal{Z}^{-1} \exp(-\mathbf{x}^T \mathbf{A}\mathbf{x}/2 + \mathbf{b}^T \mathbf{x}), \quad (11)$$

where \mathcal{Z} is a distribution normalization factor. Denoting the vector $\mu \triangleq \mathbf{A}^{-1}\mathbf{b}$, the Gaussian

density function can be rewritten as

$$\begin{aligned}
 p(\mathbf{x}) &= \mathcal{Z}^{-1} \exp(\mu^T \mathbf{A} \mu / 2) \\
 &\times \exp(-\mathbf{x}^T \mathbf{A} \mathbf{x} / 2 + \mu^T \mathbf{A} \mathbf{x} - \mu^T \mathbf{A} \mu / 2) \\
 &= \zeta^{-1} \exp(-(\mathbf{x} - \mu)^T \mathbf{A} (\mathbf{x} - \mu) / 2) \\
 &= \mathcal{N}(\mu, \mathbf{A}^{-1}), \tag{12}
 \end{aligned}$$

where the new normalization factor $\zeta \triangleq \mathcal{Z} \exp(-\mu^T \mathbf{A} \mu / 2)$. It follows that the target solution $\mathbf{x}^* = \mathbf{A}^{-1} \mathbf{b}$ is equal to $\mu \triangleq \mathbf{A}^{-1} \mathbf{b}$, the mean vector of the distribution $p(\mathbf{x})$, as defined above (11).

Hence, in order to solve the system of linear equations we need to infer the marginal densities, which must also be Gaussian, $p(x_i) \sim \mathcal{N}(\mu_i = \{\mathbf{A}^{-1} \mathbf{b}\}_i, P_i^{-1} = \{\mathbf{A}^{-1}\}_{ii})$, where μ_i and P_i are the marginal mean and inverse variance (sometimes called the precision), respectively. ■

According to Proposition 8, solving a deterministic vector-matrix linear equation translates to solving an inference problem in the corresponding graph. The move to the probabilistic domain calls for the utilization of BP as an efficient inference engine.

Remark 9: Defining a jointly Gaussian probability density function, immediately yields an implicit assumption on the positive semi-definiteness of the precision matrix \mathbf{A} , in addition to the symmetry assumption. However, we would like to stress out that this assumption emerges only for exposition purposes, so we can use the notion of ‘Gaussian probability’, but the derivation of the GaBP solver itself does not use this assumption. See the numerical example of the exact GaBP-based solution of a system with a symmetric, but not positive semi-definite, data matrix \mathbf{A} in Section VIII-C.

B. Belief Propagation

Belief propagation (BP) is equivalent to applying Pearl’s local message-passing algorithm [4], originally derived for exact inference in trees, to a general graph even if it contains cycles (loops). BP has been found to have outstanding empirical success in many applications, e.g., in decoding Turbo codes and low-density parity-check (LDPC) codes. The excellent performance of BP in these applications may be attributed to the sparsity of the graphs, which ensures that cycles in the graph are long, and inference may be performed as if it were a tree.

The BP algorithm functions by passing real-valued messages across edges in the graph and consists of two computational rules, namely the ‘sum-product rule’ and the ‘product rule’. In contrast to typical applications of BP in coding theory [17], our graphical representation resembles to a pairwise Markov random field [5] with a single type of propagating messages, rather than a factor graph [18] with two different types of messages, originated from either the variable node or the factor node. Furthermore, in most graphical model representations used in the information theory literature the graph nodes are assigned with discrete values, while in this contribution we deal with nodes corresponding to continuous variables. Thus, for a graph \mathcal{G} composed of potentials ψ_{ij} and ϕ_i as previously defined, the conventional sum-product rule becomes an integral-product rule [8] and the message $m_{ij}(x_j)$, sent from node i to node j over their shared edge on the graph, is given by

$$m_{ij}(x_j) \propto \int_{x_i} \psi_{ij}(x_i, x_j) \phi_i(x_i) \prod_{k \in \mathcal{N}(i) \setminus j} m_{ki}(x_i) dx_i. \quad (13)$$

The marginals are computed (as usual) according to the product rule

$$p(x_i) = \alpha \phi_i(x_i) \prod_{k \in \mathcal{N}(i)} m_{ki}(x_i), \quad (14)$$

where the scalar α is a normalization constant. Note that the propagating messages (and the graph potentials) do not have to describe valid (*i.e.*, normalized) density probability functions, as long as the inferred marginals do.

C. The Gaussian BP Algorithm

Gaussian BP is a special case of continuous BP, where the underlying distribution is Gaussian. Now, we derive the Gaussian BP update rules by substituting Gaussian distributions into the continuous BP update equations.

Given the data matrix \mathbf{A} and the observation vector \mathbf{b} , one can write explicitly the Gaussian density function, $p(\mathbf{x})$ (12), and its corresponding graph \mathcal{G} . Using the graph definition and a certain (arbitrary) pairwise factorization of the Gaussian function (12), the edge potentials (compatibility functions) and self potentials (‘evidence’) ϕ_i are determined to be

$$\psi_{ij}(x_i, x_j) \triangleq \exp(-x_i A_{ij} x_j), \quad (15)$$

$$\phi_i(x_i) \triangleq \exp(b_i x_i - A_{ii} x_i^2 / 2), \quad (16)$$

respectively. Note that by completing the square, one can observe that

$$\phi_i(x_i) \propto \mathcal{N}(\mu_{ii} = b_i / A_{ii}, P_{ii}^{-1} = A_{ii}^{-1}). \quad (17)$$

The graph topology is specified by the structure of the matrix \mathbf{A} , i.e. the edges set $\{i, j\}$ includes all non-zero entries of \mathbf{A} for which $i > j$.

Before describing the inference algorithm performed over the graphical model, we make the elementary but very useful observation that the product of Gaussian densities over a common variable is, up to a constant factor, also a Gaussian density.

Lemma 10: Let $f_1(x)$ and $f_2(x)$ be the probability density functions of a Gaussian random variable with two possible densities $\mathcal{N}(\mu_1, P_1^{-1})$ and $\mathcal{N}(\mu_2, P_2^{-1})$, respectively. Then their product, $f(x) = f_1(x)f_2(x)$ is, up to a constant factor, the probability density function of a Gaussian random variable with distribution $\mathcal{N}(\mu, P^{-1})$, where

$$\mu = P^{-1}(P_1\mu_1 + P_2\mu_2), \quad (18)$$

$$P^{-1} = (P_1 + P_2)^{-1}. \quad (19)$$

The proof of this lemma is found in Appendix I.

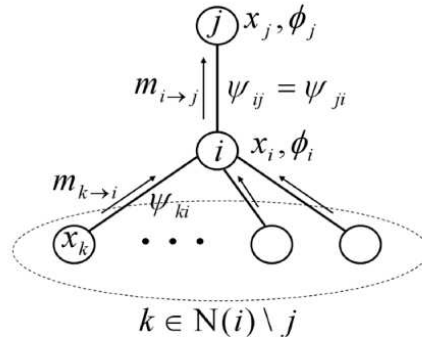


Fig. 1. Belief propagation message flow

Fig. 1 plots a portion of a certain graph, describing the neighborhood of node i . Each node (empty circle) is associated with a variable and self potential ϕ , which is a function of this variable, while edges go with the pairwise (symmetric) potentials Ψ . Messages are propagating along the edges on both directions (only the messages relevant for the computation of m_{ij} are drawn in Fig. 1). Looking at the right hand side of the integral-product rule (13), node i needs to first calculate the product of all incoming messages, except for the message coming from node j . Recall that since $p(\mathbf{x})$ is jointly Gaussian, the factorized self potentials $\phi_i(x_i) \propto \mathcal{N}(\mu_{ii}, P_{ii}^{-1})$ (17) and similarly all messages $m_{ki}(x_i) \propto \mathcal{N}(\mu_{ki}, P_{ki}^{-1})$ are of Gaussian form as well.

As the terms in the product of the incoming messages and the self potential in the integral-product rule (13) are all a function of the same variable, x_i (associated with the node i), then, according to the multivariate extension of Lemma 10,

$$\phi_i(x_i) \prod_{k \in \mathcal{N}(i) \setminus j} m_{ki}(x_i) \quad (20)$$

is proportional to a certain Gaussian distribution, $\mathcal{N}(\mu_{i \setminus j}, P_{i \setminus j}^{-1})$. Applying the multivariate version of the product precision expression in (19), the update rule for the inverse variance is given by (over-braces denote the origin of each of the terms)

$$P_{i \setminus j} = \overbrace{P_{ii}}^{\phi_i(x_i)} + \sum_{k \in \mathcal{N}(i) \setminus j} \overbrace{P_{ki}}^{m_{ki}(x_i)}, \quad (21)$$

where $P_{ii} \triangleq A_{ii}$ is the inverse variance a-priori associated with node i , via the precision of $\phi_i(x_i)$, and P_{ki} are the inverse variances of the messages $m_{ki}(x_i)$. Similarly using (18) for the multivariate case, we can calculate the mean

$$\mu_{i \setminus j} = P_{i \setminus j}^{-1} \left(\overbrace{P_{ii} \mu_{ii}}^{\phi_i(x_i)} + \sum_{k \in \mathcal{N}(i) \setminus j} \overbrace{P_{ki} \mu_{ki}}^{m_{ki}(x_i)} \right), \quad (22)$$

where $\mu_{ii} \triangleq b_i/A_{ii}$ is the mean of the self potential and μ_{ki} are the means of the incoming messages.

Next, we calculate the remaining terms of the message $m_{ij}(x_j)$, including the integration over x_i . After some algebraic manipulation (deferred to Appendix II), using the Gaussian integral

$$\int_{-\infty}^{\infty} \exp(-ax^2 + bx) dx = \sqrt{\pi/a} \exp(b^2/4a), \quad (23)$$

we find that the messages $m_{ij}(x_j)$ are proportional to normal distribution with precision and mean

$$P_{ij} = -A_{ij}^2 P_{i \setminus j}^{-1}, \quad (24)$$

$$\mu_{ij} = -P_{ij}^{-1} A_{ij} \mu_{i \setminus j}. \quad (25)$$

These two scalars represent the messages propagated in the Gaussian BP-based algorithm. Finally, computing the product rule (14) is similar to the calculation of the previous product (20) and the resulting mean (22) and precision (21), but including all incoming messages.

The marginals are inferred by normalizing the result of this product. Thus, the marginals are found to be Gaussian probability density functions $\mathcal{N}(\mu_i, P_i^{-1})$ with precision and mean

$$P_i = \overbrace{P_{ii}}^{\phi_i(x_i)} + \sum_{k \in \mathcal{N}(i)} \overbrace{P_{ki}}^{m_{ki}(x_i)}, \quad (26)$$

$$\mu_i = P_{i \setminus j}^{-1} \left(\overbrace{P_{ii} \mu_{ii}}^{\phi_i(x_i)} + \sum_{k \in \mathcal{N}(i)} \overbrace{P_{ki} \mu_{ki}}^{m_{ki}(x_i)} \right), \quad (27)$$

respectively. The derivation of the GaBP-based solver algorithm is concluded by simply substituting the explicit derived expressions of $P_{i \setminus j}$ (21) into P_{ij} (24), $\mu_{i \setminus j}$ (22) and P_{ij} (24) into μ_{ij} (25) and $P_{i \setminus j}$ (21) into μ_i (27).

The message passing in the GaBP solver can be performed subject to any scheduling. We refer to two conventional messages updating rules: parallel (flooding or synchronous) and serial (sequential, asynchronous) scheduling. In the parallel scheme, messages are stored in two data structures: messages from the previous iteration round, and messages from the current round. Thus, incoming messages do not affect the result of the computation in the current round, since it is done on messages that were received in the previous iteration round. Unlike this, in the serial scheme, there is only one data structure, so incoming messages in this round, change the result of the computation. In a sense it is exactly like the difference between the Jacobi and Gauss-Seidel algorithms, to be discussed in the following. Some in-depth discussions about parallel vs. serial scheduling in the BP context can be found in the work of Elidan *et al.* [19].

D. Max-Product Rule

A well-known alternative version to the sum-product BP is the max-product (a.k.a. min-sum) algorithm [20]. In this variant of BP, maximization operation is performed rather than marginalization, *i.e.*, variables are eliminated by taking maxima instead of sums. For Trellis trees (e.g., graphically representing convolutional codes or ISI channels), the conventional sum-product BP algorithm boils down to performing the BCJR algorithm [21], resulting in the most probable symbol, while its max-product counterpart is equivalent to the Viterbi algorithm [22], thus inferring the most probable sequence of symbols [18].

In order to derive the max-product version of the proposed GaBP solver, the integral(sum)-product rule (13) is replaced by a new rule

$$m_{ij}(x_j) \propto \arg \max_{x_i} \psi_{ij}(x_i, x_j) \phi_i(x_i) \prod_{k \in \mathcal{N}(i) \setminus j} m_{ki}(x_i) dx_i. \quad (28)$$

Algorithm 1:

1. *Initialize:*
 - ✓ Set the neighborhood $\mathcal{N}(i)$ to include $\forall k \neq i \exists A_{ki} \neq 0$.
 - ✓ Set the scalar fixes $P_{ii} = A_{ii}$ and $\mu_{ii} = b_i/A_{ii}, \forall i$.
 - ✓ Set the initial $\mathcal{N}(i) \ni k \rightarrow i$ scalar messages $P_{ki} = 0$ and $\mu_{ki} = 0$.
 - ✓ Set a convergence threshold ϵ .
2. *Iterate:*
 - ✓ Propagate the $\mathcal{N}(i) \ni k \rightarrow i$ messages P_{ki} and $\mu_{ki}, \forall i$ (under certain scheduling).
 - ✓ Compute the $\mathcal{N}(j) \ni i \rightarrow j$ scalar messages $P_{ij} = -A_{ij}^2 / (P_{ii} + \sum_{k \in \mathcal{N}(i) \setminus j} P_{ki})$,
 $\mu_{ij} = (P_{ii}\mu_{ii} + \sum_{k \in \mathcal{N}(i) \setminus j} P_{ki}\mu_{ki}) / A_{ij}$.
3. *Check:*
 - ✓ If the messages P_{ij} and μ_{ij} did not converge (w.r.t. ϵ), return to Step 2.
 - ✓ Else, continue to Step 4.
4. *Infer:*
 - ✓ Compute the marginal means $\mu_i = (P_{ii}\mu_{ii} + \sum_{k \in \mathcal{N}(i)} P_{ki}\mu_{ki}) / (P_{ii} + \sum_{k \in \mathcal{N}(i)} P_{ki}), \forall i$.
 - (✓ Optionally compute the marginal precisions $P_i = P_{ii} + \sum_{k \in \mathcal{N}(i)} P_{ki}$)
5. *Solve:*
 - ✓ Find the solution $x_i^* = \mu_i, \forall i$.

Computing $m_{ij}(x_j)$ according to this max-product rule, one gets (the exact derivation is deferred to Appendix III)

$$m_{ij}(x_j) \propto \mathcal{N}(\mu_{ij} = -P_{ij}^{-1}A_{ij}\mu_{i \setminus j}, P_{ij}^{-1} = -A_{ij}^{-2}P_{i \setminus j}), \quad (29)$$

which is identical to the messages derived for the sum-product case (24)-(25). Thus interestingly, as opposed to ordinary (discrete) BP, the following property of the GaBP solver emerges.

Corollary 11: The max-product (Eq. 28) and sum-product (Eq. 13) versions of the GaBP solver are identical.

IV. CONVERGENCE AND EXACTNESS

In ordinary BP, convergence does not entail exactness of the inferred probabilities, unless the graph has no cycles. Luckily, this is not the case for the GaBP solver. Its underlying

Gaussian nature yields a direct connection between convergence and exact inference. Moreover, in contrast to BP the convergence of GaBP is not limited for tree or sparse graphs and can occur even for dense (fully-connected) graphs, adhering to certain rules discussed in the following.

We can use results from the literature on probabilistic inference in graphical models [8]–[10] to determine the convergence and exactness properties of the GaBP-based solver. The following two theorems establish sufficient conditions under which GaBP is guaranteed to converge to the exact marginal means.

Theorem 12: [8, Claim 4] If the matrix \mathbf{A} is strictly diagonally dominant, then GaBP converges and the marginal means converge to the true means.

This sufficient condition was recently relaxed to include a wider group of matrices.

Theorem 13: [9, Proposition 2] If the spectral radius of the matrix \mathbf{A} satisfies

$$\rho(|\mathbf{I}_n - \mathbf{A}|) < 1, \quad (30)$$

then GaBP converges and the marginal means converge to the true means. (The assumption here is that the matrix \mathbf{A} is first normalized by multiplying with \mathbf{D}^{-1} , where $\mathbf{D} = \text{diag}(\mathbf{A})$.)

A third and weaker sufficient convergence condition (relative to Theorem 13) which characterizes the convergence of the variances is given in [6, Theorem 2]: For each row in the matrix \mathbf{A} , if $A_{ii}^2 > \sum_{j \neq i} A_{ij}^2$ then the variances converge. Regarding the means, additional condition related to Theorem 13 is given.

There are many examples of linear systems that violate these conditions, for which GaBP converges to the exact means. In particular, if the graph corresponding to the system is acyclic (*i.e.*, a tree), GaBP yields the exact marginal means (and variances [8]), regardless of the value of the spectral radius of the matrix [8]. Another example, where the graph is fully-connected, is discussed in the following section. However, in contrast to conventional iterative methods derived from linear algebra, understanding the conditions for exact convergence and quantifying the convergence rate of the GaBP solver remain intriguing open problems.

A. Convergence Acceleration

Further speed-up of GaBP can be achieved by adapting known acceleration techniques from linear algebra, such Aitken’s method and Steffensen’s iterations [16]. Consider a sequence $\{x_n\}$ (*e.g.*, obtained by using GaBP iterations) linearly converging to the limit \hat{x} , and $x_n \neq \hat{x}$

for $n \geq 0$. According to Aitken's method, if there exists a real number a such that $|a| < 1$ and $\lim_{n \rightarrow \infty} (x_n - \hat{x}) / (x_{n-1} - \hat{x}) = a$, then the sequence $\{y_n\}$ defined by

$$y_n = x_n - \frac{(x_{n+1} - x_n)^2}{x_{n+2} - 2x_{n+1} + x_n}$$

converges to \hat{x} faster than $\{x_n\}$ in the sense that $\lim_{n \rightarrow \infty} |(\hat{x} - y_n) / (\hat{x} - x_n)| = 0$. Aitken's method can be viewed as a generalization of over-relaxation, since one uses values from three, rather than two, consecutive iteration rounds. This method can be easily implemented in GaBP as every node computes values based only on its own history.

Steffensen's iterations incorporate Aitken's method. Starting with x_n , two iterations are run to get x_{n+1} and x_{n+2} . Next, Aitken's method is used to compute y_n , this value replaces the original x_n , and GaBP is executed again to get a new value of x_{n+1} . This process is repeated iteratively until convergence. We remark that, although the convergence rate is improved with these enhanced algorithms, the region of convergence of the accelerated GaBP solver remains unchanged.

V. COMPUTATIONAL COMPLEXITY AND MESSAGE-PASSING EFFICIENCY

For a dense matrix \mathbf{A} each node out of the n nodes sends a unique message to every other node on the fully-connected graph. This recipe results in a total of n^2 messages per iteration round.

The computational complexity of the GaBP solver as described in Algorithm 1 for a dense linear system, in terms of operations (multiplications and additions) per iteration round, is shown in Table I. In this case, the total number of required operations per iteration is $\mathcal{O}(n^3)$. This number is obtained by evaluating the number of operations required to generate a message multiplied by the number of messages. Based on the summation expressions for the propagating messages P_{ij} and μ_{ij} , it is easily seen that it takes $\mathcal{O}(n)$ operations to compute such a message. In the dense case, the graph is fully-connected resulting in $\mathcal{O}(n^2)$ propagating messages.

In order to estimate the total number of operations required for the GaBP algorithm to solve the linear system, we have to evaluate the number of iterations required for convergence. It is known [23] that the number of iterations required for an iterative solution method is $\mathcal{O}(f(\kappa))$, where $f(\kappa)$ is a function of the condition number of the data matrix \mathbf{A} . Hence the total complexity of the GaBP solver can be expressed by $\mathcal{O}(n^3) \times \mathcal{O}(f(\kappa))$. The analytical evaluation of the convergence rate function $f(\kappa)$ is a challenging open problem. However, it

Algorithm	Operations per msg	msgs	Total operations per iteration
Naive GaBP (Algorithm 1)	$\mathcal{O}(n)$	$\mathcal{O}(n^2)$	$\mathcal{O}(n^3)$
Broadcast GaBP (Algorithm 2)	$\mathcal{O}(n)$	$\mathcal{O}(n)$	$\mathcal{O}(n^2)$

TABLE I

COMPUTATIONAL COMPLEXITY OF THE GABP SOLVER FOR DENSE $n \times n$ MATRIX \mathbf{A} .

can be upper bounded by $f(\kappa) < \kappa$. furthermore, based on our experimental study, described in Section VIII, we can conclude that $f(\kappa) \leq \sqrt{\kappa}$. Thus, the total complexity of the GaBP solve in this case is $\mathcal{O}(n^3) \times \mathcal{O}(\sqrt{\kappa})$. For well-conditioned (as opposed to ill-conditioned) data matrices the condition number is $\mathcal{O}(1)$. Thus, for well-conditioned linear systems the total complexity is $\mathcal{O}(n^3)$, *i.e.*, the complexity is cubic, the same order as for direct solution methods, like Gaussian elimination.

At first sight, this result may be considered disappointing, with no complexity gain w.r.t. direct matrix inversion. Luckily, the GaBP implementation as described in Algorithm 1 is a naive one, thus termed naive GaBP. In this implementation we did not take into account the correlation between the different messages transmitted from a certain node i . These messages, computed by summation, distinct from one another in only two summation terms.

Instead of sending a message composed of the pair of μ_{ij} and P_{ij} , a node can broadcast the aggregated sums

$$\tilde{P}_i = P_{ii} + \sum_{k \in \mathcal{N}(i)} P_{ki}, \quad (31)$$

$$\tilde{\mu}_i = \tilde{P}_i^{-1} (P_{ii}\mu_{ii} + \sum_{k \in \mathcal{N}(i)} P_{ki}\mu_{ki}). \quad (32)$$

Consequently, each node can retrieve locally the $P_{i \setminus j}$ (21) and $\mu_{i \setminus j}$ (22) from the sums by means of a subtraction

$$P_{i \setminus j} = \tilde{P}_i - P_{ji}, \quad (33)$$

$$\mu_{i \setminus j} = \tilde{\mu}_i - P_{i \setminus j}^{-1} P_{ji} \mu_{ji}. \quad (34)$$

The rest of the algorithm remains the same. On dense graphs, the broadcast version sends $\mathcal{O}(n)$ messages per round, instead of $\mathcal{O}(n^2)$ messages in the GaBP algorithm.

Algorithm 2:

1. <i>Initialize:</i>	<ul style="list-style-type: none"> ✓ Set the neighborhood $\mathcal{N}(i)$ to include $\forall k \neq i \exists A_{ki} \neq 0$. ✓ Set the scalar fixes $P_{ii} = A_{ii}$ and $\mu_{ii} = b_i/A_{ii}, \forall i$. ✓ Set the initial $i \rightarrow \mathcal{N}(i)$ broadcast messages $\tilde{P}_i = 0$ and $\tilde{\mu}_i = 0$. ✓ Set the initial $\mathcal{N}(i) \ni k \rightarrow i$ internal scalars $P_{ki} = 0$ and $\mu_{ki} = 0$. ✓ Set a convergence threshold ϵ.
2. <i>Iterate:</i>	<ul style="list-style-type: none"> ✓ Broadcast the aggregated sum messages $\tilde{P}_i = P_{ii} + \sum_{k \in \mathcal{N}(i)} P_{ki}$, $\tilde{\mu}_i = \tilde{P}_i^{-1} (P_{ii}\mu_{ii} + \sum_{k \in \mathcal{N}(i)} P_{ki}\mu_{ki}), \forall i$ (under certain scheduling). ✓ Compute the $\mathcal{N}(j) \ni i \rightarrow j$ internal scalars $P_{ij} = -A_{ij}^2/(\tilde{P}_i - P_{ji})$, $\mu_{ij} = (\tilde{P}_i\tilde{\mu}_i - P_{ji}\mu_{ji})/A_{ij}$.
3. <i>Check:</i>	<ul style="list-style-type: none"> ✓ If the internal scalars P_{ij} and μ_{ij} did not converge (w.r.t. ϵ), return to Step 2. ✓ Else, continue to Step 4.
4. <i>Infer:</i>	<ul style="list-style-type: none"> ✓ Compute the marginal means $\mu_i = (P_{ii}\mu_{ii} + \sum_{k \in \mathcal{N}(i)} P_{ki}\mu_{ki})/(P_{ii} + \sum_{k \in \mathcal{N}(i)} P_{ki}) = \tilde{\mu}_i, \forall i$. (✓ Optionally compute the marginal precisions $P_i = P_{ii} + \sum_{k \in \mathcal{N}(i)} P_{ki} = \tilde{P}_i$)
5. <i>Solve:</i>	<ul style="list-style-type: none"> ✓ Find the solution $x_i^* = \mu_i, \forall i$.

VI. THE GABP-BASED SOLVER AND CLASSICAL SOLUTION METHODS

A. Gaussian Elimination

Proposition 14: The GaBP-based solver (Algorithm 1) for a system of linear equations represented by a tree graph is identical to the renowned Gaussian elimination algorithm (a.k.a. LU factorization, [23]).

Proof: **[Proof]** Consider a set of n linear equations with n unknown variables, a unique solution and a tree graph representation. We aim at computing the unknown variable associated with the root node. Without loss of generality as the tree can be drawn with any of the other nodes being its root. Let us enumerate the nodes in an ascending order from the root to the leaves (see, e.g., Fig. 2).

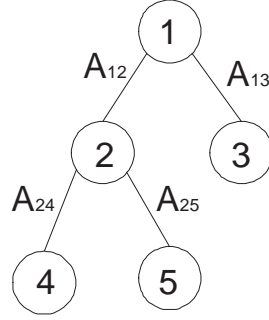


Fig. 2. Example topology of a tree with 5 nodes

As in a tree each child node (*i.e.*, all nodes but the root) has only one parent node and based on the top-down ordering, it can be easily observed that the tree graph's corresponding data matrix \mathbf{A} must have one and only one non-zero entry in the upper triangular portion of its columns. Moreover, for a leaf node this upper triangular entry is the only non-zero off-diagonal entry in the whole column. See, for example, the data matrix associated with the tree graph depicted in Fig 2

$$\begin{pmatrix} A_{11} & \mathbf{A_{12}} & \underline{\mathbf{A_{13}}} & 0 & 0 \\ A_{12} & A_{22} & 0 & \underline{\mathbf{A_{24}}} & \underline{\mathbf{A_{25}}} \\ A_{13} & 0 & A_{33} & 0 & 0 \\ 0 & A_{24} & 0 & A_{44} & 0 \\ 0 & A_{25} & 0 & 0 & A_{55} \end{pmatrix}, \quad (35)$$

where the non-zero upper triangular entries are in bold and among these the entries corresponding to leaves are underlined.

Now, according to GE we would like to lower triangulate the matrix \mathbf{A} . This is done by eliminating these entries from the leaves to the root. Let l be a leaf node, i be its parent and j be its parent (l 'th node grandparent). Then, the l 'th row is multiplied by $-A_{li}/A_{ll}$ and added to the i 'th row. in this way the A_{li} entry is being eliminated. However, this elimination, transforms the i 'th diagonal entry to be $A_{ii} \rightarrow A_{ii} - A_{li}^2/A_{ll}$, or for multiple leaves connected to the same parent $A_{ii} \rightarrow A_{ii} - \sum_{l \in \mathcal{N}(i)} A_{li}^2/A_{ll}$. In our example,

$$\begin{pmatrix} A_{11} & A_{12} & 0 & 0 & 0 \\ A_{12} & A_{22} - A_{13}^2/A_{33} - A_{24}^2/A_{44} - A_{25}^2/A_{55} & 0 & 0 & 0 \\ A_{13} & 0 & A_{33} & 0 & 0 \\ 0 & A_{24} & 0 & A_{44} & 0 \\ 0 & A_{25} & 0 & 0 & A_{55} \end{pmatrix}. \quad (36)$$

Thus, in a similar manner, eliminating the parent i yields the multiplication of the j 'th diagonal term by $-A_{ij}^2/(A_{ii} - \sum_{l \in \mathcal{N}(i)} A_{li}^2/A_{ll})$. Recalling that $P_{ii} = A_{ii}$, we see that the last expression is identical to the update rule of P_{ij} in GaBP. Again, in our example

$$\begin{pmatrix} B & 0 & 0 & 0 & 0 \\ 0 & C & 0 & 0 & 0 \\ A_{13} & 0 & A_{33} & 0 & 0 \\ 0 & A_{24} & 0 & A_{44} & 0 \\ 0 & A_{25} & 0 & 0 & A_{55} \end{pmatrix}, \quad (37)$$

where $B = A_{11} - A_{12}^2/(A_{22} - A_{13}^2/A_{33} - A_{24}^2/A_{44} - A_{25}^2/A_{55})$, $C = A_{22} - A_{13}^2/A_{33} - A_{24}^2/A_{44} - A_{25}^2/A_{55}$. Now the matrix is fully lower triangulated. To put differently in terms of GaBP, the P_{ij} messages are subtracted from the diagonal P_{ii} terms to triangulate the data matrix of the tree. Performing the same row operations on the right hand side column vector \mathbf{b} , it can be easily seen that we equivalently get that the outcome of the row operations is identical to the GaBP solver's μ_{ij} update rule. These updates/row operations can be repeated, in the general case, until the matrix is lower triangulated.

Now, in order to compute the value of the unknown variable associated with the root node, all we have to do is divide the first diagonal term by the transformed value of b_1 , which is identical to the infer stage in the GaBP solver (note that by definition all the nodes connected to the root are its children, as it does not have parent node). In the example

$$x_1^* = \frac{A_{11} - A_{12}^2/(A_{22} - A_{13}^2/A_{33} - A_{24}^2/A_{44} - A_{25}^2/A_{55})}{b_{11} - A_{12}/(b_{22} - A_{13}/A_{33} - A_{24}/A_{44} - A_{25}/A_{55})} \quad (38)$$

Note that the rows corresponding to leaves remain unchanged.

To conclude, in the tree graph case, the 'iterative' stage (stage 2 on algorithm 1) of the GaBP solver actually performs lower triangulation of the matrix, while the 'infer' stage (stage 4) reduces to what is known as forward substitution. Evidently, using an opposite ordering, one can get the complementary upper triangulation and back substitution, respectively. ■

It is important to note, that based on this proposition, the GaBP solver can be viewed as GE ran over an unwrapped version (i.e., a computation tree) of a general loopy graph.

B. Iterative Methods

Iterative methods that can be expressed in the simple form

$$\mathbf{x}^{(t)} = \mathbf{B}\mathbf{x}^{(t-1)} + \mathbf{c}, \quad (39)$$

where neither the iteration matrix \mathbf{B} nor the vector \mathbf{c} depend upon the iteration number t , are called stationary iterative methods. In the following, we discuss three main stationary iterative methods: the Jacobi method, the Gauss-Seidel (GS) method and the successive overrelaxation (SOR) method. The GaBP-based solver, in the general case, can not be written in this form, thus can not be categorized as a stationary iterative method.

Proposition 15: [23] Assuming $\mathbf{I} - \mathbf{B}$ is invertible, then the iteration 39 converges (for any initial guess, $\mathbf{x}^{(0)}$).

C. Jacobi Method

The Jacobi method (Gauss, 1823, and Jacobi 1845, [2]), a.k.a. the simultaneous iteration method, is the oldest iterative method for solving a square linear system of equations $\mathbf{A}\mathbf{x} = \mathbf{b}$. The method assumes that $\forall_i A_{ii} \neq 0$. It's complexity is $\mathcal{O}(n^2)$ per iteration. A sufficient convergence condition for the Jacobi method is that for any starting vector \mathbf{x}_0 as long as $\rho(\mathbf{D}^{-1}(\mathbf{L} + \mathbf{U})) < 1$. Where $\mathbf{D} = \text{diag}\{\mathbf{A}\}$, \mathbf{L}, \mathbf{U} are upper and lower triangular matrices of \mathbf{A} . A second sufficient convergence condition is that \mathbf{A} is diagonally dominant.

Proposition 16: The GaBP-based solver (Algorithm 1)

- 1) with inverse variance messages arbitrarily set to zero, i.e., $P_{ij} = 0, i \in \mathbf{N}(j), \forall j$;
- 2) incorporating the message received from node j when computing the message to be sent from node i to node j , i.e. replacing $k \in \mathbf{N}(i) \setminus j$ with $k \in \mathbf{N}(i)$,

is identical to the Jacobi iterative method.

Proof: [**Proof**] Arbitrarily setting the precisions to zero, we get in correspondence to the above derivation,

$$P_{i \setminus j} = P_{ii} = A_{ii}, \quad (40)$$

$$P_{ij} \mu_{ij} = -A_{ij} \mu_{i \setminus j}, \quad (41)$$

$$\mu_i = A_{ii}^{-1} (b_i - \sum_{k \in \mathbf{N}(i)} A_{ki} \mu_{k \setminus i}). \quad (42)$$

Note that the inverse relation between P_{ij} and $P_{i \setminus j}$ (24) is no longer valid in this case.

Now, we rewrite the mean $\mu_{i \setminus j}$ (22) without excluding the information from node j ,

$$\mu_{i \setminus j} = A_{ii}^{-1} (b_i - \sum_{k \in \mathbf{N}(i)} A_{ki} \mu_{k \setminus i}). \quad (43)$$

Note that $\mu_{i \setminus j} = \mu_i$, hence the inferred marginal mean μ_i (42) can be rewritten as

$$\mu_i = A_{ii}^{-1} (b_i - \sum_{k \neq i} A_{ki} \mu_k), \quad (44)$$

where the expression for all neighbors of node i is replaced by the redundant, yet identical, expression $k \neq i$. This fixed-point iteration is identical to the renowned Jacobi method, concluding the proof. ■

Proposition 16 can be viewed also as a probabilistic proof of Jacobi. The fact that Jacobi iterations can be obtained as a special case of the GaBP solver further indicates the richness of the proposed algorithm. Note, that the GaBP algorithm converges to the exact solution also for nonsymmetric matrices in this form.

D. Gauss-Seidel

The Gauss-Seidel method converges for any starting vector \mathbf{x}_0 if $\rho((\mathbf{L} + \mathbf{D})^{-1}\mathbf{U}) < 1$.

This condition holds, for example, for diagonally dominant matrices as well as for positive definite ones. It is necessary, however, that the diagonal terms in the matrix are greater (in magnitude) than the other terms.

The successive overrelaxation (SOR) method aims to further refine the Gauss-Seidel method, by adding a damping parameter $0 < \alpha < 1$:

$$x_i^t = \alpha x_i^{t-1} + (1 - \alpha)GS_i, \quad (45)$$

where GS_i is the Gauss-Seidel update computed by node i . Damping has previously shown to be a heuristic for accelerating belief propagation as well [24].

VII. DISTRIBUTED ITERATIVE COMPUTATION OF MOORE-PENROSE PSEUDOINVERSE

In this section, we efficiently extend the applicability of the proposed GaBP-based solver for systems with symmetric matrices to systems with any square (*i.e.*, also nonsymmetric) or rectangular matrix. We first construct a new symmetric data matrix $\tilde{\mathbf{R}}$ based on an arbitrary (non-rectangular) matrix $\mathbf{S} \in \mathbb{R}^{k \times n}$

$$\tilde{\mathbf{R}} \triangleq \begin{pmatrix} \mathbf{I}_k & \mathbf{S}^T \\ \mathbf{S} & -\Psi \end{pmatrix} \in \mathbb{R}^{(k+n) \times (k+n)}. \quad (46)$$

Additionally, we define a new vector of variables $\tilde{\mathbf{x}} \triangleq \{\hat{\mathbf{x}}^T, \mathbf{z}^T\}^T \in \mathbb{R}^{(k+n) \times 1}$, where $\hat{\mathbf{x}} \in \mathbb{R}^{k \times 1}$ is the (to be shown) solution vector and $\mathbf{z} \in \mathbb{R}^{n \times 1}$ is an auxiliary hidden vector, and a new observation vector $\tilde{\mathbf{y}} \triangleq \{\mathbf{0}^T, \mathbf{y}^T\}^T \in \mathbb{R}^{(k+n) \times 1}$.

Now, we would like to show that solving the symmetric linear system $\tilde{\mathbf{R}}\tilde{\mathbf{x}} = \tilde{\mathbf{y}}$, taking the first k entries of the corresponding solution vector $\tilde{\mathbf{x}}$ is equivalent to solving the original (not necessarily symmetric) system $\mathbf{R}\mathbf{x} = \mathbf{y}$. Note that in the new construction the matrix $\tilde{\mathbf{R}}$

is sparse again, and has only $2nk$ off-diagonal nonzero elements. When running the GaBP algorithm we have only $2nk$ messages, instead of n^2 in the previous construction.

Writing explicitly the symmetric linear system's equations, we get

$$\begin{aligned}\hat{\mathbf{x}} + \mathbf{S}^T \mathbf{z} &= \mathbf{0}, \\ \mathbf{S} \hat{\mathbf{x}} - \Psi \mathbf{z} &= \mathbf{y}.\end{aligned}$$

Thus,

$$\hat{\mathbf{x}} = \Psi \mathbf{S}^T (\mathbf{y} - \mathbf{S} \hat{\mathbf{x}}),$$

and extracting $\hat{\mathbf{x}}$ we have

$$\hat{\mathbf{x}} = (\mathbf{S}^T \mathbf{S} + \Psi_n)^{-1} \mathbf{S}^T \mathbf{y}.$$

Note, that when the noise level is zero, $\Psi = 0_{m \times m}$, we get the Moore-Penrose pseudoinverse solution

$$\hat{\mathbf{x}} = (\mathbf{S}^T \mathbf{S})^{-1} \mathbf{S}^T \mathbf{y} = \mathbf{S}^\dagger \mathbf{y}.$$

VIII. NUMERICAL EXAMPLES AND APPLICATIONS

Our experimental study includes four numerical examples and two possible applications. In all examples, but the Poisson's equation 58, \mathbf{b} is assumed to be an m -length all-ones observation vector. For fairness in comparison, the initial guess in all experiments, for the various solution methods under investigation, is taken to be the same and is arbitrarily set to be equal to the value of the vector \mathbf{b} . The stopping criterion in all experiments determines that for all propagating messages (in the context the GaBP solver) or all n tentative solutions (in the context of the compared iterative methods) the absolute value of the difference should be less than $\epsilon \leq 10^{-6}$. As for terminology, in the following performing GaBP with parallel (flooding or synchronous) message scheduling is termed 'parallel GaBP', while GaBP with serial (sequential or asynchronous) message scheduling is termed 'serial GaBP'.

A. Numerical Example: Toy Linear System: 3×3 Equations

Consider the following 3×3 linear system

$$\underbrace{\begin{pmatrix} A_{xx} = 1 & A_{xy} = -2 & A_{xz} = 3 \\ A_{yx} = -2 & A_{yy} = 1 & A_{yz} = 0 \\ A_{zx} = 3 & A_{zy} = 0 & A_{zz} = 1 \end{pmatrix}}_{\mathbf{A}} \underbrace{\begin{pmatrix} x \\ y \\ z \end{pmatrix}}_{\mathbf{x}} = \underbrace{\begin{pmatrix} -6 \\ 0 \\ 2 \end{pmatrix}}_{\mathbf{b}}. \quad (47)$$

We would like to find the solution to this system, $\mathbf{x}^* = \{x^*, y^*, z^*\}^T$. Inverting the data matrix \mathbf{A} , we directly solve

$$\underbrace{\begin{pmatrix} x^* \\ y^* \\ z^* \end{pmatrix}}_{\mathbf{x}^*} = \underbrace{\begin{pmatrix} -1/12 & -1/6 & 1/4 \\ -1/6 & 2/3 & 1/2 \\ 1/4 & 1/2 & 1/4 \end{pmatrix}}_{\mathbf{A}^{-1}} \underbrace{\begin{pmatrix} -6 \\ 0 \\ 2 \end{pmatrix}}_{\mathbf{b}} = \begin{pmatrix} 1 \\ 2 \\ -1 \end{pmatrix}. \quad (48)$$

Alternatively, we can now run the GaBP solver. Fig. 3 displays the graph, corresponding to the data matrix \mathbf{A} , and the message-passing flow. As $A_{yz} = A_{zy} = 0$, this graph is a cycle-free tree, thus GaBP is guaranteed to converge in a finite number of rounds. As demonstrated in the following, in this example GaBP converges only in two rounds, which equals the tree's diameter. Each propagating message, m_{ij} , is described by two scalars μ_{ij} and P_{ij} , standing for the mean and precision of this distribution. The evolution of the propagating means and precisions, until convergence, is described in Table VIII-A, where the notation $t = 0, 1, 2, 3$ denotes the iteration rounds. Converged values are written in bold.

Message	Computation	t=0	t=1	t=2	t=3
P_{xy}	$-A_{xy}^2/(P_{xx} + P_{zx})$	0	-4	1/2	1/2
P_{yx}	$-A_{yx}^2/(P_{yy})$	0	-4	-4	-4
P_{xz}	$-A_{xz}^2/(P_{zz})$	0	-9	3	3
P_{zx}	$-A_{zx}^2/(P_{xx} + P_{yx})$	0	-9	-9	-9
μ_{xy}	$(P_{xx}\mu_{xx} + P_{zx}\mu_{zx})/A_{xy}$	0	3	6	6
μ_{yx}	$P_{yy}\mu_{yy}/A_{yx}$	0	0	0	0
μ_{xz}	$(P_{xx}\mu_{xx} + P_{yx}\mu_{yx})/A_{xz}$	0	-2	-2	-2
μ_{zx}	$P_{zz}\mu_{zz}/A_{zx}$	0	2/3	2/3	2/3

TABLE II

EVOLUTION OF MEANS AND PRECISIONS ON A TREE WITH THREE NODES

Next, following the GaBP solver algorithm, we infer the marginal means. For exposition purposes we also present in Table III the tentative solutions at each iteration round.

Thus, as expected, the GaBP solution $\mathbf{x}^* = \{x^* = 1, y^* = 2, z^* = -1\}^T$ is identical to what is found taking the direct approach. Note that as the linear system is described by a

Solution	Computation	t=0	t=1	t=2	t=3
μ_x	$(P_{xx}\mu_{xx} + P_{zx}\mu_{zx} + P_{yx}\mu_{yx})/(P_{xx} + P_{zx} + P_{yx})$	-6	1	1	1
μ_y	$(P_{yy}\mu_{yy} + P_{xy}\mu_{xy})/(P_{yy} + P_{xy})$	0	4	2	2
μ_z	$(P_{zz}\mu_{zz} + P_{xz}\mu_{xz})/(P_{zz} + P_{xz})$	2	-5/2	-1	-1

TABLE III

TENTATIVE MEANS COMPUTED ON EACH ITERATION UNTIL CONVERGENCE

tree graph, then for this particular case, the inferred precision is also exact

$$P_x = P_{xx} + P_{yx} + P_{zx} = -12, \quad (49)$$

$$P_y = P_{yy} + P_{xy} = 3/2, \quad (50)$$

$$P_z = P_{zz} + P_{xz} = 4. \quad (51)$$

$$(52)$$

and gives $\{P_x^{-1} = \{\mathbf{A}^{-1}\}_{xx} = -1/12, P_y^{-1} = \{\mathbf{A}^{-1}\}_{yy} = 2/3, P_z^{-1} = \{\mathbf{A}^{-1}\}_{zz} = 1/4\}^T$, i.e. the true diagonal values of the data matrix's inverse, \mathbf{A}^{-1} .

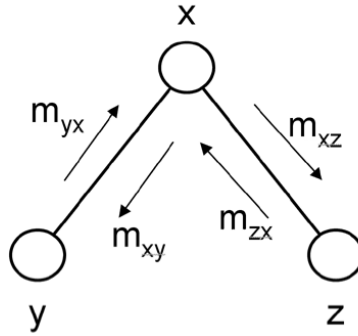


Fig. 3. A tree topology with three nodes

B. Application Example: Linear Detection

Consider a discrete-time channel with a real input vector $\mathbf{x} = \{x_1, \dots, x_K\}^T$ governed by an arbitrary prior distribution, $P_{\mathbf{x}}$, and a corresponding real output vector $\mathbf{y} = \{y_1, \dots, y_K\}^T = f\{\mathbf{x}^T\} \in \mathbb{R}^K$.³ Here, the function $f\{\cdot\}$ denotes the channel transformation. By definition,

³An extension to the complex domain is straightforward.

linear detection compels the decision rule to be

$$\hat{\mathbf{x}} = \Delta\{\mathbf{x}^*\} = \Delta\{\mathbf{A}^{-1}\mathbf{b}\}, \quad (53)$$

where $\mathbf{b} = \mathbf{y}$ is the $K \times 1$ observation vector and the $K \times K$ matrix \mathbf{A} is a positive-definite symmetric matrix approximating the channel transformation. The vector \mathbf{x}^* is the solution (over \mathbb{R}) to $\mathbf{A}\mathbf{x} = \mathbf{b}$. Estimation is completed by adjusting the (inverse) matrix-vector product to the input alphabet, dictated by $P_{\mathbf{x}}$, accomplished by using a proper clipping function $\Delta\{\cdot\}$ (e.g., for binary signaling $\Delta\{\cdot\}$ is the sign function).

For example, linear channels, which appear extensively in many applications in communication and data storage systems, are characterized by the linear relation

$$\mathbf{y} = f\{\mathbf{x}\} = \mathbf{R}\mathbf{x} + \mathbf{n}, \quad (54)$$

where \mathbf{n} is a $K \times 1$ additive noise vector and $\mathbf{R} = \mathbf{S}^T\mathbf{S}$ is a positive-definite symmetric matrix, often known as the correlation matrix. The $N \times K$ matrix \mathbf{S} describes the physical channel medium while the vector \mathbf{y} corresponds to the output of a bank of filters matched to the physical channel \mathbf{S} .

Due to the vast applicability of linear channels, in Section VIII we focus in our experimental study on such channels, although our paradigm is not limited to this case. Assuming linear channels with AWGN with variance σ^2 as the ambient noise, the general linear detection rule (53) can describe known linear detectors. For example [25], [26]:

- The conventional matched filter (MF) detector is obtained by taking $\mathbf{A} \triangleq \mathbf{I}_K$ and $\mathbf{b} = \mathbf{y}$. This detector is optimal, in the MAP-sense, for the case of zero cross-correlations, *i.e.*, $\mathbf{R} = \mathbf{I}_K$, as happens for orthogonal CDMA or when there is no ISI effect.
- The decorrelator (zero forcing equalizer) is achieved by substituting $\mathbf{A} \triangleq \mathbf{R}$ and $\mathbf{b} = \mathbf{y}$. It is optimal in the noiseless case.
- The linear minimum mean-square error (MMSE) detector can also be described by using $\mathbf{A} = \mathbf{R} + \sigma^2\mathbf{I}_K$ and $\mathbf{b} = \mathbf{y}$. This detector is known to be optimal when the input distribution $P_{\mathbf{x}}$ is Gaussian.

In general, linear detection is suboptimal because of its deterministic underlying mechanism (*i.e.*, solving a given set of linear equations), in contrast to other estimation schemes, such as MAP or maximum likelihood, that emerge from an optimization criterion. In the following section we implement the linear detection operation, in its general form (53), in an efficient message-passing fashion.

The essence of detection theory is to estimate a hidden input to a channel from empirically-observed outputs. An important class of practical sub-optimal detectors is based on linear detection. This class includes, for instance, the conventional single-user matched filter, the decorrelator (also, called the zero-forcing equalizer), the linear minimum mean-square error (MMSE) detector, and many other detectors with widespread applicability [25], [26]. In general terms, given a probabilistic estimation problem, linear detection solves a deterministic system of linear equations derived from the original problem, thereby providing a sub-optimal, but often useful, estimate of the unknown input.

Applying the GaBP solver to linear detection, we establish a new and explicit link between BP and linear detection. This link strengthens the connection between message-passing inference and estimation theory, previously seen in the context of optimal maximum a-posteriori (MAP) detection [27], [28] and several sub-optimal nonlinear detection techniques [29] applied in the context of both dense and sparse [30], [31] graphical models.

In the following experimental study, we examine the implementation of a decorrelator detector in a noiseless synchronous CDMA system with binary signaling and spreading codes based upon Gold sequences of length $m = 7$.⁴ Two system setups are simulated, corresponding to $n = 3$ and $n = 4$ users, resulting in the cross-correlation matrices

$$\mathbf{R}_3 = \frac{1}{7} \begin{pmatrix} 7 & -1 & 3 \\ -1 & 7 & -5 \\ 3 & -5 & 7 \end{pmatrix} \quad (55)$$

and

$$\mathbf{R}_4 = \frac{1}{7} \begin{pmatrix} 7 & -1 & 3 & 3 \\ -1 & 7 & 3 & -1 \\ 3 & 3 & 7 & -1 \\ 3 & -1 & -1 & 7 \end{pmatrix}, \quad (56)$$

respectively.⁵

The decorrelator detector, a member of the family of linear detectors, solves a system of linear equations, $\mathbf{A}\mathbf{x} = \mathbf{b}$, where the matrix \mathbf{A} is equal to the $n \times n$ correlation matrix \mathbf{R} , and the observation vector \mathbf{b} is identical to the n -length CDMA channel output vector \mathbf{y} .

⁴In this case, as long as the system is not overloaded, *i.e.* the number of active users n is not greater than the spreading code's length m , the decorrelator detector yields optimal detection decisions.

⁵These particular correlation settings were taken from the simulation setup of Yener *et al.* [15].

Thus the vector of decorrelator decisions is determined by taking the signum of the vector $\mathbf{A}^{-1}\mathbf{b} = \mathbf{R}^{-1}\mathbf{y}$. Note that \mathbf{R}_3 and \mathbf{R}_4 are not strictly diagonally dominant, but their spectral radii are less than unity, since $\rho(|\mathbf{I}_3 - \mathbf{R}_3|) = 0.9008 < 1$ and $\rho(|\mathbf{I}_4 - \mathbf{R}_4|) = 0.8747 < 1$, respectively. In all of the experiments, we assumed the output vector was the all-ones vector.

Table IV compares the proposed GaBP algorithm with standard iterative solution methods [2] (using random initial guesses), previously employed for CDMA multiuser detectors (MUD). Specifically, MUD algorithms based on the algorithms of Jacobi, Gauss-Seidel (GS) and (optimally weighted) successive over-relaxation (SOR)⁶ were investigated [13], [14]. The table lists the convergence rates for the two Gold code-based CDMA settings. Convergence is identified and declared when the differences in all the iterated values are less than 10^{-6} . We see that, in comparison with the previously proposed detectors based upon the Jacobi and GS algorithms, the GaBP detectors converge more rapidly for both $n = 3$ and $n = 4$. The serial (asynchronous) GaBP algorithm achieves the best overall convergence rate, surpassing even the SOR-based detector.

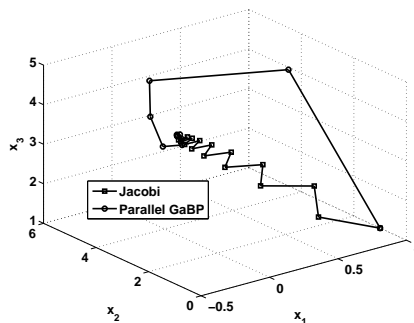


Fig. 4. Convergence of the GaBP algorithm vs. Jacobi on a 3×3 gold CDMA matrix. Each dimension shows one coordinate of the solution. Jacobi converges in zigzags while GaBP has spiral convergence.

Further speed-up of GaBP can be achieved by adapting known acceleration techniques from linear algebra, such Aitken's method and Steffensen's iterations [16]. Consider a sequence $\{x_n\}$ (e.g., obtained by using GaBP iterations) linearly converging to the limit \hat{x} , and $x_n \neq \hat{x}$ for $n \geq 0$. According to Aitken's method, if there exists a real number a such that $|a| < 1$

⁶This moving average improvement of Jacobi and GS algorithms is equivalent to what is known in the BP literature as 'damping' [24].

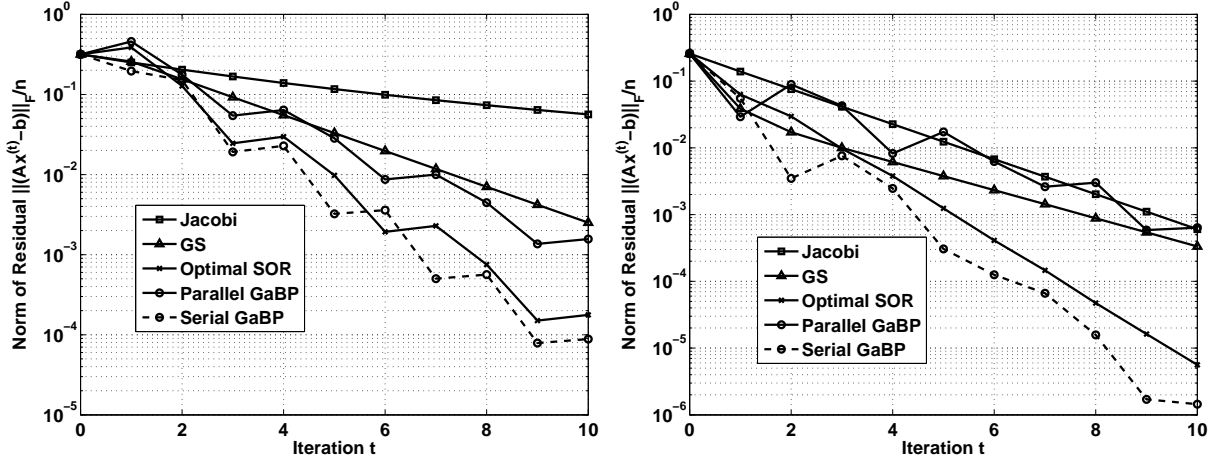


Fig. 5. Convergence of the two gold CDMA matrices. To the left \mathbf{R}_3 , to the right, \mathbf{R}_4 .

Algorithm	Iterations t (\mathbf{R}_3)	Iterations t (\mathbf{R}_4)
Jacobi	111	24
GS	26	26
Parallel GaBP	23	24
Optimal SOR	17	14
Serial GaBP	16	13

TABLE IV

DECORRELATOR FOR $K = 3, 4$ -USER, $N = 7$ GOLD CODE CDMA. TOTAL NUMBER OF ITERATIONS REQUIRED FOR CONVERGENCE (THRESHOLD $\epsilon = 10^{-6}$) FOR GABP-BASED SOLVERS VS. STANDARD METHODS.

and $\lim_{n \rightarrow \infty} (x_n - \hat{x}) / (x_{n-1} - \hat{x}) = a$, then the sequence $\{y_n\}$ defined by

$$y_n = x_n - \frac{(x_{n+1} - x_n)^2}{x_{n+2} - 2x_{n+1} + x_n}$$

converges to \hat{x} faster than $\{x_n\}$ in the sense that $\lim_{n \rightarrow \infty} |(\hat{x} - y_n) / (\hat{x} - x_n)| = 0$. Aitken's method can be viewed as a generalization of over-relaxation, since one uses values from three, rather than two, consecutive iteration rounds. This method can be easily implemented in GaBP as every node computes values based only on its own history.

Algorithm	R ₃	R ₄
Jacobi+Steffensen ⁷	59	—
Parallel GaBP+Steffensen	13	13
Serial GaBP+Steffensen	9	7

TABLE V

DECORRELATOR FOR $K = 3, 4$ -USER, $N = 7$ GOLD CODE CDMA. TOTAL NUMBER OF ITERATIONS REQUIRED FOR CONVERGENCE (THRESHOLD $\epsilon = 10^{-6}$) FOR JACOBI, PARALLEL AND SERIAL GABP SOLVERS ACCELERATED BY STEFFENSEN ITERATIONS.

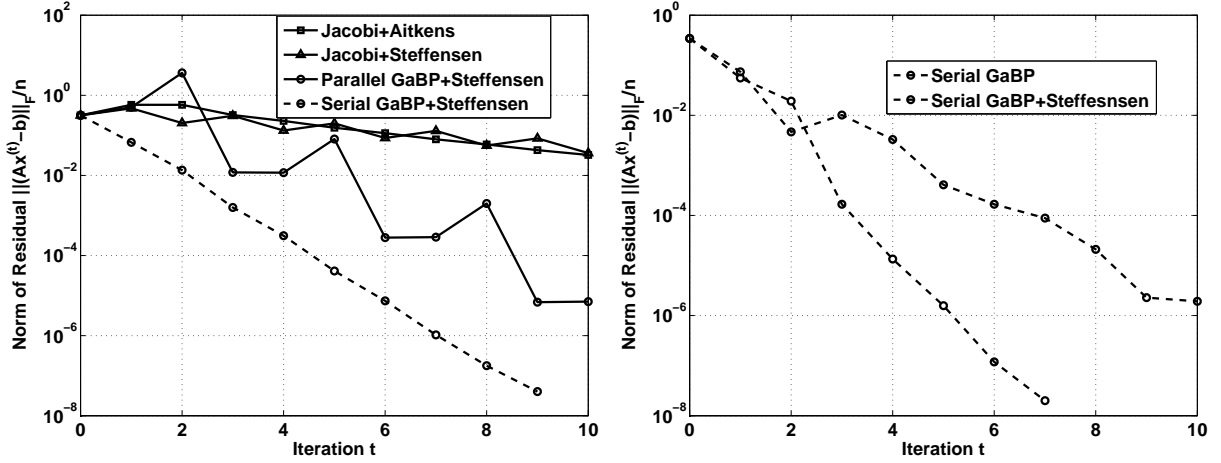


Fig. 6. Convergence acceleration of the GaBP algorithm using Aitken and Steffensen methods. The left graph depicts a 3×3 gold CDMA matrix, the right graph 4×4 gold CDMA matrix. Further details regarding simulation setup are found in Section VIII-B.

Steffensen's iterations incorporate Aitken's method. Starting with x_n , two iterations are run to get x_{n+1} and x_{n+2} . Next, Aitken's method is used to compute y_n , this value replaces the original x_n , and GaBP is executed again to get a new value of x_{n+1} . This process is repeated iteratively until convergence. Table V demonstrates the speed-up of GaBP obtained by using these acceleration methods, in comparison with that achieved by the similarly modified Jacobi

algorithm.⁸ We remark that, although the convergence rate is improved with these enhanced algorithms, the region of convergence of the accelerated GaBP solver remains unchanged.

For the algorithms we examined, Fig. 1-(a) displays the Euclidean distance between the tentative (intermediate) results and the fixed-point solution as a function of the number of iterations. As expected, all linear algorithms exhibit a logarithmic convergence behaviour. Note that GaBP converges faster on average, although there are some fluctuations in the GaBP curves, in contrast to the monotonicity of the other curves.

An interesting question concerns the origin of this convergence speed-up associated with GaBP. Better understanding may be gained by visualizing the iterations of the different methods for the matrix \mathbf{R}_3 case. The convergence contours are plotted in the space of $\{x_1, x_2, x_3\}$ in Fig. 1-(b). As expected, the Jacobi algorithm converges in zigzags towards the fixed point (this behavior is well-explained in Bertsekas and Tsitsiklis [23]). The fastest algorithm is serial GaBP. It is interesting to note that GaBP convergence is in a spiral shape, hinting that despite the overall convergence improvement, performance improvement is not guaranteed in successive iteration rounds. The spiral nature of GaBP convergence is better viewed in Fig. 1-(c). In this case the system was simulated with a specific \mathbf{R} matrix for which Jacobi algorithm and other standard methods did not even converge. Using Aitken's method, a further speed-up in GaBP convergence was obtained.

Despite the fact that the examples considered correspond to small multi-user systems, we believe that the results reflect the typical behavior of the algorithms, and that similar qualitative results would be observed in larger systems. In support of this belief, we note, in passing, that GaBP was experimentally shown to converge in a logarithmic number of iterations in the cases of very large matrices both dense (with up to hundreds of thousands of dimensions [33]) and sparse (with up to millions of dimensions [34], [35]).

As a final remark on the linear detection example, we mention that, in the case of a channel with Gaussian input signals, for which linear detection is optimal, it can be easily shown that the proposed GaBP scheme reduces to the BP-based MUD scheme, recently introduced by Montanari *et al.* [36]. Their BP scheme, tailored specifically for Gaussian signaling, has been proven to converge to the MMSE (and optimal) solution for any arbitrarily loaded,

⁸Application of Aitken and Steffensen's methods for speeding-up the convergence of standard (non-BP) iterative solution algorithms in the context of MUD was introduced by Leibig *et al.* [32].

randomly-spread CDMA system (*i.e.*, a system where $\rho(\mathbf{I}_n - \mathbf{R}) \lesssim 1$).⁹ Thus Gaussian-input additive white Gaussian noise CDMA is another example for which the proposed GaBP solver converges to the MAP decisions for any $m \times n$ random spreading matrix \mathbf{S} , regardless of the spectral radius.

C. Numerical Example: Symmetric Non-PSD Indefinite) Data Matrix

Consider the case of a linear system with a symmetric, but non-PSD data matrix

$$\begin{pmatrix} 1 & 2 & 3 \\ 2 & 2 & 1 \\ 3 & 1 & 1 \end{pmatrix}. \quad (57)$$

Table VI displays the number of iterations required for convergence for the iterative methods under consideration. The classical methods diverge, even when aided with acceleration techniques. This behavior (at least without the acceleration) is not surprising in light of Theorem 13. Again we observe that serial scheduling of the GaBP solver is superior parallel scheduling and that applying Steffensen iterations reduces the number of iterations in 45% in both cases. Note that SOR cannot be defined when the matrix is not PSD. By definition CG works only for symmetric PSD matrices. because the solution is a saddle point and not a minimum or maximum.

IX. APPLICATION EXAMPLE: 2-D POISSON'S EQUATION

One of the most common partial differential equations (PDEs) encountered in various areas of exact sciences and engineering (*e.g.*, heat flow, electrostatics, gravity, fluid flow, quantum mechanics, elasticity) is Poisson's equation. In two dimensions, the equation is

$$\Delta u(x, y) = f(x, y), \quad (58)$$

for $\{x, y\} \in \Omega$, where

$$\Delta(\cdot) = \frac{\partial^2(\cdot)}{\partial x^2} + \frac{\partial^2(\cdot)}{\partial y^2}. \quad (59)$$

is the Laplacean operator and Ω is a bounded domain in \mathbb{R}^2 . The solution is well defined only under boundary conditions, *i.e.*, the value of $u(x, y)$ on the boundary of Ω is specified. We consider the simple (Dirichlet) case of $u(x, y) = 0$ for $\{x, y\}$ on the boundary of Ω . This

⁹For non-Gaussian signaling, *e.g.* with binary input alphabet, this BP-based detector is conjectured to converge only in the large-system limit, as $n, m \rightarrow \infty$ [36].

Algorithm	Iterations t
Jacobi,GS,SR,Jacobi+Aitkens,Jacobi+Steffensen	—
Parallel GaBP	38
Serial GaBP	25
Parallel GaBP+Steffensen	21
Serial GaBP+Steffensen	14

TABLE VI

SYMMETRIC NON-PSD 3×3 DATA MATRIX. TOTAL NUMBER OF ITERATIONS REQUIRED FOR CONVERGENCE
(THRESHOLD $\epsilon = 10^{-6}$) FOR GABP-BASED SOLVERS VS. STANDARD METHODS.

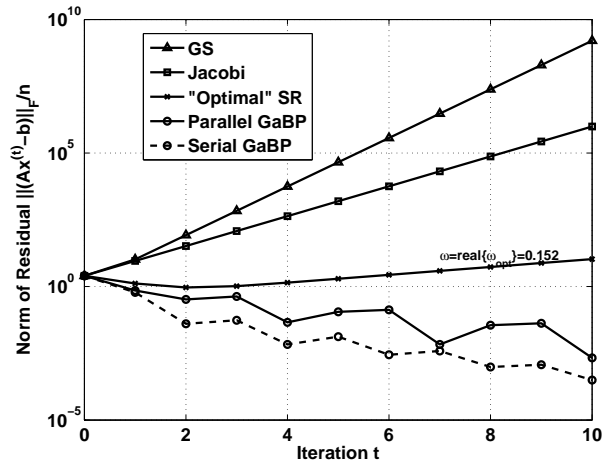


Fig. 7. Convergence rate for a 3×3 symmetric non-PSD data matrix. The Frobenius norm of the residual per equation, $\|\mathbf{Ax}^t - b\|_F/n$, as a function of the iteration t for GS (triangles and solid line), Jacobi (squares and solid line), SR (stars and solid line), parallel GaBP (circles and solid line) and serial GaBP (circles and dashed line) solvers.

equation describes, for instance, the steady-state temperature of a uniform square plate with the boundaries held at temperature $u = 0$, and $f(x, y)$ equaling the external heat supplied at point $\{x, y\}$.

The poisson's PDE can be discretized by using finite differences. An $p + 1 \times p + 1$ square grid on Ω with size (arbitrarily) set to unity is used, where $h \triangleq 1/(p + 1)$ is the grid spacing.

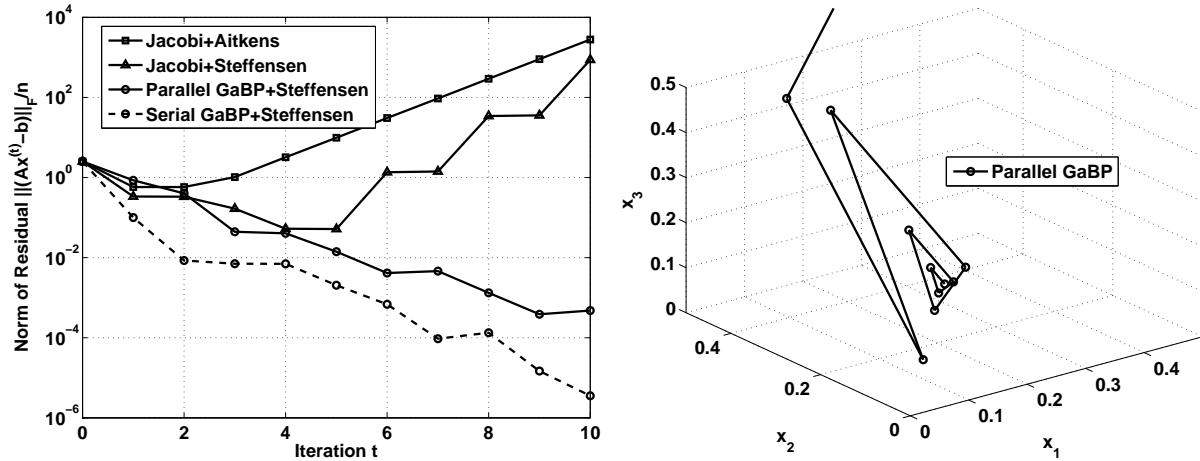


Fig. 8. The left graph depicts accelerated convergence rate for a 3×3 symmetric non-PSD data matrix. The Frobenius norm of the residual per equation, $\|Ax^t - b\|_F/n$, as a function of the iteration t for Aitkens (squares and solid line) and Steffensen-accelerated (triangles and solid line) Jacobi method, parallel GaBP (circles and solid line) and serial GaBP (circles and dashed line) solvers accelerated by Steffensen iterations. The right graph shows a visualization of parallel GaBP on the same problem, drawn in \mathbb{R}^3 .

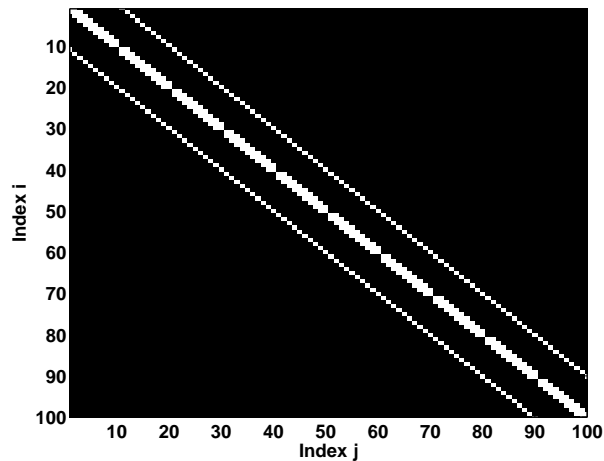


Fig. 9. Image of the corresponding sparse data matrix for the 2-D discrete Poisson's PDE with $p = 10$. Empty (full) squares denote non-zero (zero) entries.

We let $U(i, j)$, $\{i, j = 0, \dots, p + 1\}$, be the approximate solution to the PDE at $x = ih$ and

$y = jh$. Approximating the Laplacean by

$$\begin{aligned} \Delta U(x, y) &= \frac{\partial^2(U(x, y))}{\partial x^2} + \frac{\partial^2(U(x, y))}{\partial y^2} \\ &\approx \frac{U(i+1, j) - 2U(i, j) + U(i-1, j)}{h^2} + \frac{U(i, j+1) - 2U(i, j) + U(i, j-1)}{h^2} \end{aligned} \quad (60)$$

one gets the system of $n = p^2$ linear equations with n unknowns

$$4U(i, j) - U(i-1, j) - U(i+1, j) - U(i, j-1) - U(i, j+1) = b(i, j) \forall i, j = 1, \dots, p, \quad (61)$$

where $b(i, j) \triangleq -f(ih, jh)h^2$, the scaled value of the function $f(x, y)$ at the corresponding grid point $\{i, j\}$. Evidently, the accuracy of this approximation to the PDE increases with n .

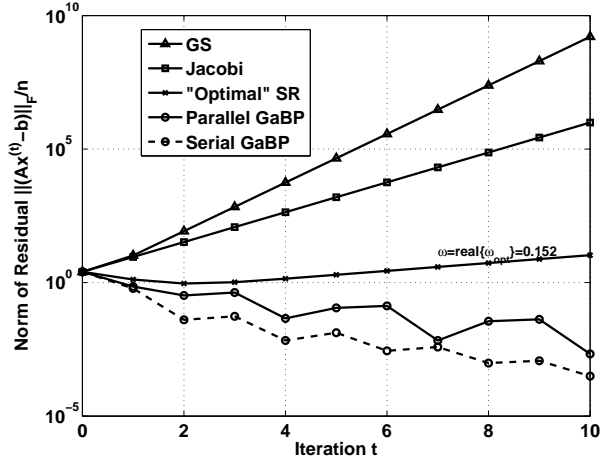


Fig. 10. Convergence rate for a 3×3 symmetric non-PSD data matrix. The Frobenius norm of the residual per equation, $\|\mathbf{Ax}^t - b\|_F/n$, as a function of the iteration t for GS (triangles and solid line), Jacobi (squares and solid line), SR (stars and solid line), parallel GaBP (circles and solid line) and serial GaBP (circles and dashed line) solvers.

Choosing a certain ordering of the unknowns $U(i, j)$, the linear system can be written in a matrix-vector form. For example, the natural row ordering (*i.e.*, enumerating the grid points left→right, bottom→up) leads to a linear system with $p^2 \times p^2$ sparse data matrix \mathbf{A} . For

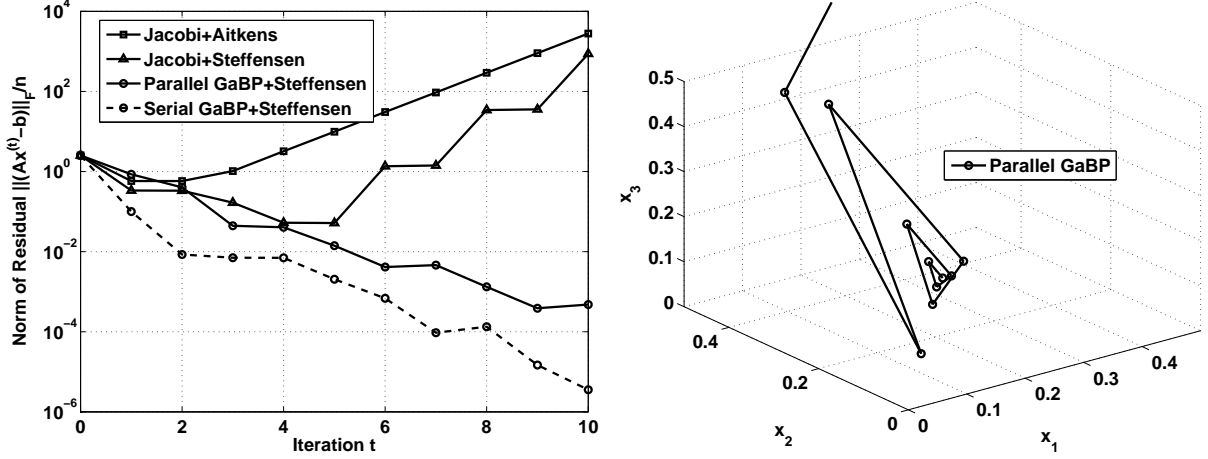


Fig. 11. The left graph depicts accelerated convergence rate for a 3×3 symmetric non-PSD data matrix. The Frobenius norm of the residual per equation, $\|Ax^t - b\|_F/n$, as a function of the iteration t for Aitkens (squares and solid line) and Steffensen-accelerated (triangles and solid line) Jacobi method, parallel GaBP (circles and solid line) and serial GaBP (circles and dashed line) solvers accelerated by Steffensen iterations. The right graph shows a visualization of parallel GaBP on the same problem, drawn in \mathbb{R}^3 .

example, a Poisson PDE with $p = 3$ generates the following 9×9 linear system

$$\underbrace{\begin{pmatrix} 4 & -1 & & & & & & & \\ -1 & 4 & -1 & & & & & & \\ & -1 & 4 & & & & & & \\ \hline -1 & & & 4 & -1 & & & & \\ & -1 & & -1 & 4 & -1 & & & \\ & & -1 & & -1 & 4 & & & -1 \\ \hline & & & -1 & & & 4 & -1 & \\ & & & & -1 & & -1 & 4 & -1 \\ & & & & & -1 & & -1 & 4 \end{pmatrix}}_{\mathbf{A}} \underbrace{\begin{pmatrix} U(1,1) \\ U(2,1) \\ U(3,1) \\ U(1,2) \\ U(2,2) \\ U(3,2) \\ U(1,3) \\ U(2,3) \\ U(3,3) \end{pmatrix}}_{\mathbf{x}} = \underbrace{\begin{pmatrix} b(1,1) \\ b(2,1) \\ b(3,1) \\ b(1,2) \\ b(2,2) \\ b(3,2) \\ b(1,3) \\ b(2,3) \\ b(3,3) \end{pmatrix}}_{\mathbf{b}}, \quad (62)$$

where blank data matrix \mathbf{A} entries denote zeros.

Hence, now we can solve the discretized 2-D Poisson's PDE by utilizing the GaBP algorithm. Note that, in contrast to the other examples, in this case the GaBP solver is applied for solving a sparse, rather than dense, system of linear equations.

In order to evaluate the performance of the GaBP solver, we choose to solve the 2-D Poisson's equation with discretization of $p = 10$. The structure of the corresponding 100×100

Algorithm	Iterations t
Jacobi	354
GS	136
Optimal SOR	37
Parallel GaBP	134
Serial GaBP	73
Parallel GaBP+Aitkens	25
Parallel GaBP+Steffensen	56
Serial GaBP+Steffensen	32

TABLE VII

2-D DISCRETE POISSON'S PDE WITH $p = 3$ AND $f(x, y) = -1$. TOTAL NUMBER OF ITERATIONS REQUIRED FOR CONVERGENCE (THRESHOLD $\epsilon = 10^{-6}$) FOR GABP-BASED SOLVERS VS. STANDARD METHODS.

sparse data matrix is illustrated in Fig. 9.

X. CONCLUSION AND FUTURE DIRECTIONS

In this paper, we have established a powerful new connection between the problem of solving a system of linear equations and probabilistic inference on a suitable Gaussian graphical model. Exploiting this connection, we have developed an iterative, message-passing algorithm based upon Gaussian BP that can be used as a low-complexity alternative to linear algebraic solutions based upon direct matrix inversion. By its nature, the new algorithm allows an efficient, distributed implementation.

There are numerous applications in mathematics and engineering to which the new GaBP-based algorithm is applicable. We illustrated its potential performance advantages in the context of linear detection [7], [12], but many other techniques in digital communications requiring matrix inversion or determinant computation, such as channel precoding [37], are

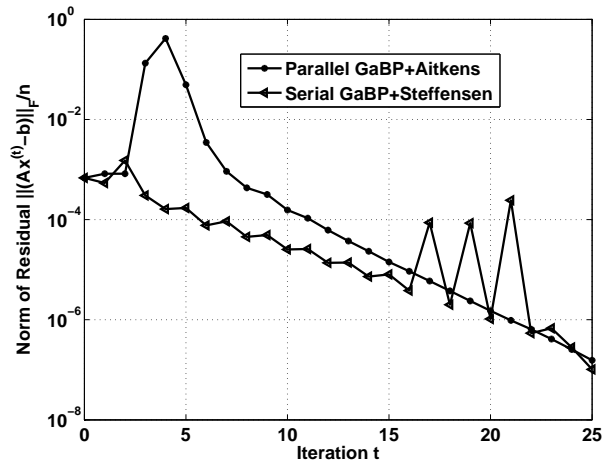


Fig. 12. Accelerated convergence rate for the 2-D discrete Poisson's PDE with $p = 10$ and $f(x, y) = -1$. The Frobenius norm of the residual, per equation, $\|\mathbf{Ax}^t - b\|_F/n$, as a function of the iteration t for parallel GaBP solver accelerated by Aitkens method (o-marks and solid line) and serial GaBP solver accelerated by Steffensen iterations (left triangles and solid line)

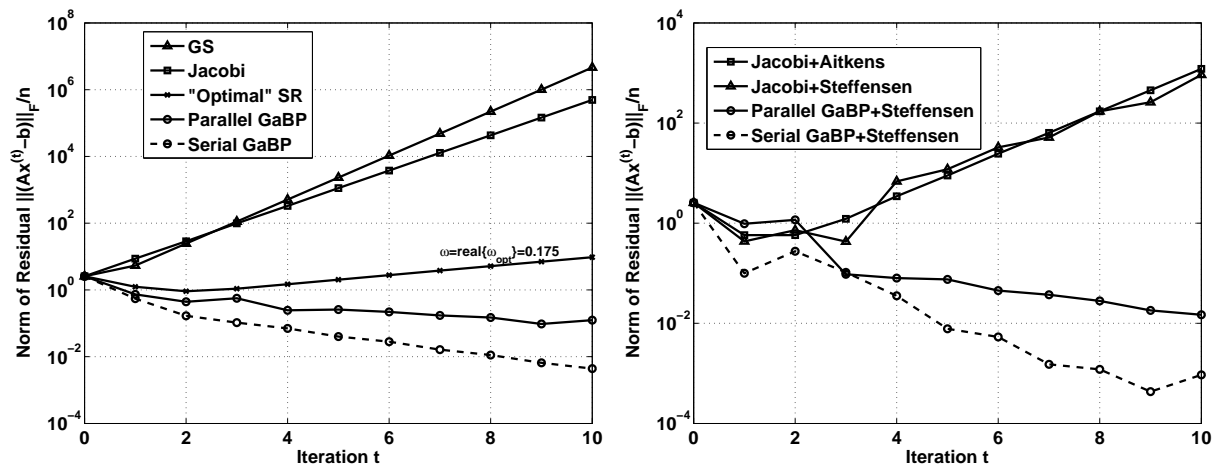


Fig. 13. Convergence of an asymmetric 3×3 matrix.

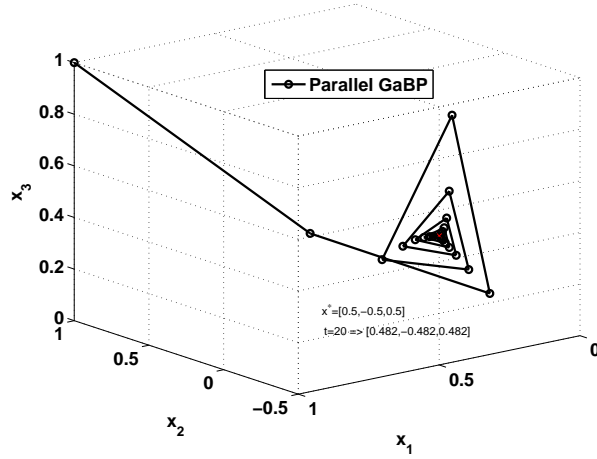
amenable to the new approach.

The extension of this technique to systems of linear equations over finite fields would open up a wealth of other applications. For example, such a development could lead to an iterative, message-passing algorithm for efficient decoding of algebraic error-correcting codes, like the widely-used class of BCH and Reed-Solomon codes.

Algorithm	Iterations t
Jacobi,GS,SR,Jacobi+Aitkens,Jacobi+Steffensen	—
Parallel GaBP	84
Serial GaBP	30
Parallel GaBP+Steffensen	43
Serial GaBP+Steffensen	17

TABLE VIII

ASYMMETRIC 3×3 DATA MATRIX. TOTAL NUMBER OF ITERATIONS REQUIRED FOR CONVERGENCE (THRESHOLD $\epsilon = 10^{-6}$) FOR GABP-BASED SOLVERS VS. STANDARD METHODS.

Fig. 14. Convergence of a 3×3 asymmetric matrix, using 3D plot.

APPENDIX I

PROOF OF LEMMA 10

Proof: Taking the product of the two Gaussian probability density functions

$$f_1(x)f_2(x) = \frac{\sqrt{P_1P_2}}{2\pi} \exp\left(-\frac{(P_1(x-\mu_1)^2 + P_2(x-\mu_2)^2)}{2}\right) \quad (63)$$

and completing the square, one gets

$$f_1(x)f_2(x) = \frac{C\sqrt{P}}{2\pi} \exp\left(-\frac{P(x-\mu)^2}{2}\right), \quad (64)$$

with

$$P \triangleq P_1 + P_2, \quad (65)$$

$$\mu \triangleq P^{-1}(\mu_1 P_1 + \mu_2 P_2) \quad (66)$$

and the scalar constant determined by

$$C \triangleq \sqrt{\frac{P}{P_1 P_2}} \exp\left(\left(P_1 \mu_1^2 (P^{-1} P_1 - 1) + P_2 \mu_2^2 (P^{-1} P_2 - 1) + 2P^{-1} P_1 P_2 \mu_1 \mu_2\right)/2\right). \quad (67)$$

Hence, the product of the two Gaussian densities is $C \cdot \mathcal{N}(\mu, P^{-1})$. \blacksquare

APPENDIX II

INTEGRATING OVER x_i

Proof:

$$m_{ij}(x_j) \propto \int_{x_i} \psi_{ij}(x_i, x_j) \phi_i(x_i) \prod_{k \in \mathcal{N}(i) \setminus j} m_{ki}(x_i) dx_i \quad (68)$$

$$\propto \int_{x_i} \overbrace{\exp(-x_i A_{ij} x_j)}^{\psi_{ij}(x_i, x_j)} \overbrace{\exp(-P_{i \setminus j} (x_i^2/2 - \mu_{i \setminus j} x_i))}^{\phi_i(x_i) \prod_{k \in \mathcal{N}(i) \setminus j} m_{ki}(x_i)} dx_i \quad (69)$$

$$= \int_{x_i} \exp\left(\left(-P_{i \setminus j} x_i^2/2\right) + (P_{i \setminus j} \mu_{i \setminus j} - A_{ij} x_j) x_i\right) dx_i \quad (70)$$

$$\propto \exp\left(\left(P_{i \setminus j} \mu_{i \setminus j} - A_{ij} x_j\right)^2 / (2P_{i \setminus j})\right) \quad (71)$$

$$\propto \mathcal{N}(\mu_{ij} = -P_{ij}^{-1} A_{ij} \mu_{i \setminus j}, P_{ij}^{-1} = -A_{ij}^{-2} P_{i \setminus j}^{-1}), \quad (72)$$

where the exponent (71) is obtained by using the Gaussian integral (23). \blacksquare

APPENDIX III

MAXIMIZING OVER x_i

Proof:

$$m_{ij}(x_j) \propto \arg \max_{x_i} \psi_{ij}(x_i, x_j) \phi_i(x_i) \prod_{k \in \mathcal{N}(i) \setminus j} m_{ki}(x_i) \quad (73)$$

$$\propto \arg \max_{x_i} \overbrace{\exp(-x_i A_{ij} x_j)}^{\psi_{ij}(x_i, x_j)} \overbrace{\exp(-P_{i \setminus j} (x_i^2/2 - \mu_{i \setminus j} x_i))}^{\phi_i(x_i) \prod_{k \in \mathcal{N}(i) \setminus j} m_{ki}(x_i)} \quad (74)$$

$$= \arg \max_{x_i} \exp\left(\left(-P_{i \setminus j} x_i^2/2\right) + (P_{i \setminus j} \mu_{i \setminus j} - A_{ij} x_j) x_i\right). \quad (75)$$

Hence, x_i^{\max} , the value of x_i maximizing the product $\psi_{ij}(x_i, x_j)\phi_i(x_i)\prod_{k\in N(i)\setminus j}m_{ki}(x_i)$ is given by equating its derivative w.r.t. x_i to zero, yielding

$$x_i^{\max} = \frac{P_{i\setminus j}\mu_{i\setminus j} - A_{ij}x_j}{P_{i\setminus j}}. \quad (76)$$

Substituting x_i^{\max} back into the product, we get

$$m_{ij}(x_j) \propto \exp((P_{i\setminus j}\mu_{i\setminus j} - A_{ij}x_j)^2/(2P_{i\setminus j})) \quad (77)$$

$$\propto \mathcal{N}(\mu_{ij} = -P_{ij}^{-1}A_{ij}\mu_{i\setminus j}, P_{ij}^{-1} = -A_{ij}^{-2}P_{i\setminus j}), \quad (78)$$

which is identical to the result obtained when eliminating x_i via integration (72). \blacksquare

APPENDIX IV

QUADRATIC MIN-SUM MESSAGE PASSING ALGORITHM

The quadratic Min-Sum message passing algorithm was initially presented in [6]. It is a variant of the max-product algorithm, with underlying Gaussian distributions. The quadratic Min-Sum algorithm is an iterative algorithm for solving a quadratic cost function. Not surprisingly, as we have shown in Section III-D that the Max-Product and the Sum-Product algorithms are identical when the underlying distributions are Gaussians. In this contribution, we show that the quadratic Min-Sum algorithm is identical to the GaBP algorithm, although it was derived differently.

In [6] the authors discuss the application for solving linear system of equations using the Min-Sum algorithm. Our work [7] was done in parallel to their work, where both papers appeared in the 45th Allerton conference.

Theorem 17: The Quadratic Min-Sum algorithm is an instance of the GaBP algorithm.

Proof: **[Proof] We start in the quadratic parameter updates:**

$$\gamma_{ij} = \frac{1}{1 - \sum_{u\in N(i)\setminus j}\Gamma_{ui}^2\gamma_{ui}} = \overbrace{\left(\underbrace{1}_{A_{ii}} - \sum_{u\in N(i)\setminus j} \underbrace{\Gamma_{ui}}_{A_{ui}} \underbrace{\gamma_{ui}}_{\substack{P_{ui}^{-1} \\ \Gamma_{iu}}} \right)^{-1}}^{P_{i\setminus j}^{-1}}$$

Which is equivalent to 21. Regarding the mean parameters,

$$z_{ij} = \frac{\Gamma_{ij}}{1 - \sum_{u\in N(i)\setminus j}\Gamma_{ui}^2\gamma_{ui}}(h_i - \sum_{u\in N(i)\setminus j}z_{ui}) = \overbrace{\left(\underbrace{\Gamma_{ij}}_{A_{ij}} \underbrace{\gamma_{ij}}_{(P_{i\setminus j})^{-1}} \underbrace{\left(\underbrace{h_i}_{b_i} - \sum_{u\in N(i)\setminus j}z_{ui} \right)}_{\mu_{i\setminus j}} \right)}^{\mu_{i\setminus j}}$$

Which is equivalent to 22. \blacksquare

TABLE IX
NOTATIONS OF MIN-SUM [6] VS. GABP

Min-Sum [6]	GaBP [7]	comments
$\gamma_{ij}^{(t+1)}$	$P_{i \setminus j}^{-1}$	quadratic parameters / product rule precision from i to j
$z_{ij}^{(t+1)}$	$\mu_{i \setminus j}$	linear parameters / product rule mean rom i to j
h_i	b_i	prior mean of node i
A_{ii}	1	prior precision of node i
x_i	x_i	posterior mean of node i
—	P_i	posterior precision of node i
Γ_{ij}	A_{ij}	covariance of nodes i and j

For simplicity of notations, we list the different notations in Min-Sum paper vs. our notations: As shown above, the Min-Sum algorithm assumes the covariance matrix Γ is first normalized s.t. the main diagonal entries (the variances) are all one. The messages sent in the Min-Sum algorithm are called linear parameters (which are equivalent to the mean messages in GaBP) and quadratic parameters (which are equivalent to variances). The difference between the algorithm is that in the GaBP algorithm, a node computes the product rule and the integral, and sends the result to its neighbor. In the Min-Sum algorithm, a node computes the product rule, sends the intermediate result, and the receiving node computes the integral. In other words, the same computation is performed but on different locations. In the Min-Sum algorithm terminology, the messages are linear and quadratic parameters vs. Gaussians in our terminology.

REFERENCES

- [1] G. H. Golub and C. F. V. Loan, Eds., *Matrix Computation*, 3rd ed. The Johns Hopkins University Press, 1996.
- [2] O. Axelsson, *Iterative Solution Methods*. Cambridge, UK: Cambridge University Press, 1994.
- [3] Y. Saad, Ed., *Iterative methods for Sparse Linear Systems*. PWS Publishing company, 1996.
- [4] J. Pearl, *Probabilistic Reasoning in Intelligent Systems: Networks of Plausible Inference*. San Francisco: Morgan Kaufmann, 1988.
- [5] M. I. Jordan, Ed., *Learning in Graphical Models*. Cambridge, MA: The MIT Press, 1999.
- [6] C. Moallemi and B. V. Roy, "Convergence of the min-sum algorithm for convex optimization," in *Proc. of the 45th Allerton Conference on Communication, Control and Computing*, Monticello, IL, September 2007.
- [7] D. Bickson, O. Shental, P. H. Siegel, J. K. Wolf, and D. Dolev, "Linear detection via belief propagation," in *Proc. 45th Allerton Conf. on Communications, Control and Computing*, Monticello, IL, USA, Sep. 2007.
- [8] Y. Weiss and W. T. Freeman, "Correctness of belief propagation in Gaussian graphical models of arbitrary topology," *Neural Computation*, vol. 13, no. 10, pp. 2173–2200, 2001.

- [9] J. K. Johnson, D. M. Malioutov, and A. S. Willsky, "Walk-sum interpretation and analysis of Gaussian belief propagation," in *Advances in Neural Information Processing Systems 18*, Y. Weiss, B. Schölkopf, and J. Platt, Eds. Cambridge, MA: MIT Press, 2006, pp. 579–586.
- [10] D. M. Malioutov, J. K. Johnson, and A. S. Willsky, "Walk-sums and belief propagation in Gaussian graphical models," *Journal of Machine Learning Research*, vol. 7, Oct. 2006.
- [11] O. Shental, P. H. S. D. Bickson, J. K. Wolf, and D. Dolev, "Gaussian belief propagation solver for systems of linear equations," in *IEEE Int. Symp. on Inform. Theory (ISIT)*, Toronto, Canada, July 2008.
- [12] D. Bickson, O. Shental, P. H. Siegel, J. K. Wolf, and D. Dolev, "Gaussian belief propagation based multiuser detection," in *IEEE Int. Symp. on Inform. Theory (ISIT)*, Toronto, Canada, July 2008.
- [13] A. Grant and C. Schlegel, "Iterative implementations for linear multiuser detectors," *IEEE Trans. Commun.*, vol. 49, no. 10, pp. 1824–1834, Oct. 2001.
- [14] P. H. Tan and L. K. Rasmussen, "Linear interference cancellation in CDMA based on iterative techniques for linear equation systems," *IEEE Trans. Commun.*, vol. 48, no. 12, pp. 2099–2108, Dec. 2000.
- [15] A. Yener, R. D. Yates, , and S. Ulukus, "CDMA multiuser detection: A nonlinear programming approach," *IEEE Trans. Commun.*, vol. 50, no. 6, pp. 1016–1024, Jun. 2002.
- [16] P. Henrici, *Elements of Numerical Analysis*. John Wiley and Sons, 1964.
- [17] S. M. Aji and R. J. McEliece, "The generalized distributive law," *IEEE Trans. Inf. Theory*, vol. 46, no. 2, pp. 325–343, Mar. 2000.
- [18] F. Kschischang, B. Frey, and H. A. Loeliger, "Factor graphs and the sum-product algorithm," *IEEE Trans. Inf. Theory*, vol. 47, pp. 498–519, Feb. 2001.
- [19] G. Elidan, McGraw, and D. Koller, "Residual belief propagation: Informed scheduling for asynchronous message passing," July 2006.
- [20] Y. Weiss and W. T. Freeman, "On the optimality of solutions of the max-product belief-propagation algorithm in arbitrary graphs," in *Information Theory, IEEE Transactions on*, vol. 47, no. 2, 2001, pp. 736–744.
- [21] L. R. Bahl, J. Cocke, F. Jelinek, and J. Raviv, "Optimal decoding of linear codes for minimizing symbol error rate," *IEEE Trans. Inf. Theory*, vol. 20, no. 3, pp. 284–287, Mar. 1974.
- [22] A. Viterbi, "Error bounds for convolutional codes and an asymptotically optimum decoding algorithm," in *Information Theory, IEEE Transactions on*, vol. 13, no. 2, 1967, pp. 260–269.
- [23] D. P. Bertsekas and J. N. Tsitsiklis, *Parallel and Distributed Calculation. Numerical Methods*. Prentice Hall, 1989.
- [24] K. M. Murphy, Y. Weiss, and M. I. Jordan, "Loopy belief propagation for approximate inference: An empirical study," in *Proc. of UAI*, 1999.
- [25] S. Verdú, *Multiuser Detection*. Cambridge, UK: Cambridge University Press, 1998.
- [26] J. G. Proakis, *Digital Communications*, 4th ed. New York, USA: McGraw-Hill, 2000.
- [27] Y. Kabashima, "A CDMA multiuser detection algorithm on the basis of belief propagation," *J. Phys. A: Math. Gen.*, vol. 36, pp. 11 111–11 121, Oct. 2003.
- [28] O. Shental, N. Shental, A. J. Weiss, and Y. Weiss, "Generalized belief propagation receiver for near-optimal detection of two-dimensional channels with memory," in *Proc. IEEE Information Theory Workshop (ITW)*, San Antonio, Texas, USA, Oct. 2004.
- [29] T. Tanaka and M. Okada, "Approximate belief propagation, density evolution, and statistical neurodynamics for CDMA multiuser detection," *IEEE Trans. Inf. Theory*, vol. 51, no. 2, pp. 700–706, Feb. 2005.
- [30] A. Montanari and D. Tse, "Analysis of belief propagation for non-linear problems: The example of CDMA (or: How to prove Tanaka's formula)," in *Proc. IEEE Inform. Theory Workshop (ITW)*, Punta del Este, Uruguay, Mar. 2006.

- [31] C. C. Wang and D. Guo, "Belief propagation is asymptotically equivalent to MAP detection for sparse linear systems," in *Proc. 44th Allerton Conf. on Communications, Control and Computing*, Monticello, IL, USA, Sep. 2006.
- [32] C. Leibig, A. Dekorsy, and J. Fliege, "Power control using Steffensen iterations for CDMA systems with beamforming or multiuser detection," in *Proc. IEEE International Conference on Communications (ICC)*, Seoul, Korea, 2005.
- [33] D. Bickson, D. Dolev, and E. Yom-Tov, "A gaussian belief propagation solver for large scale support vector machines," in *5th European Conference on Complex Systems*, Jerusalem, Sept. 2008.
- [34] D. Bickson, D. Malkhi, and L. Zhou, "Peer-to-Peer rating," in *7th IEEE P2P computing*, Galway, Ireland, 2007.
- [35] D. Bickson and D. Malkhi, "A unifying framework for rating users and data items in peer-to-peer and social networks," in *Peer-to-Peer Networking and Applications (PPNA) Journal*, Springer-Verlag, April 2008.
- [36] A. Montanari, B. Prabhakar, and D. Tse, "Belief propagation based multi-user detection," in *Proc. 43th Allerton Conf. on Communications, Control and Computing*, Monticello, IL, USA, Sep. 2005.
- [37] B. R. Vojčić and W. M. Jang, "Transmitter precoding in synchronous multiuser communications," *IEEE Trans. Commun.*, vol. 46, no. 10, pp. 1346–1355, Oct. 1998.